

Hamiltonian Description of Composite Fermions: Magnetoexciton Dispersions

Ganpathy Murthy

Physics Department, Boston University, Boston MA 02215

and Department of Physics and Astronomy, Johns Hopkins University, Baltimore MD 21218

(November 12, 2018)

A microscopic Hamiltonian theory of the FQHE, developed by Shankar and myself based on the fermionic Chern-Simons approach, has recently been quite successful in calculating gaps in Fractional Quantum Hall states, and in predicting approximate scaling relations between the gaps of different fractions. I now apply this formalism towards computing magnetoexciton dispersions (including spin-flip dispersions) in the $\nu = \frac{1}{3}$, $\frac{2}{5}$, and $\frac{3}{7}$ gapped fractions, and find approximate agreement with numerical results. I also analyse the evolution of these dispersions with increasing sample thickness, modelled by a potential soft at high momenta. New results are obtained for instabilities as a function of thickness for $\frac{2}{5}$ and $\frac{3}{7}$, and it is shown that the spin-polarized $\frac{2}{5}$ state, in contrast to the spin-polarized $\frac{1}{3}$ state, cannot be described as a simple quantum ferromagnet.

73.50.Jt, 05.30.-d, 74.20.-z

I. INTRODUCTION

The Fractional Quantum Hall (FQH) effect¹ has introduced us to new states of electrons in high magnetic fields. Seminal theoretical progress was made by Laughlin², who showed that for filling fractions $\nu = 1/(2p+1)$ the electrons form a strongly correlated state which is incompressible, and has quasiparticle excitations with fractional charge² $e^* = e/(2p+1)$. Subsequently the excitations were also shown to have fractional statistics³.

A unified understanding of all fractions $\nu = p/(2sp+1)$ was achieved by the Composite Fermion picture of Jain⁴. In this picture, the true quasiparticles are electrons dressed by $2s$ vortices, which are called Composite Fermions (CFs). At a mean field level, the CFs then see a reduced field $B^* = B/(2sp+1)$, in which they fill p CF-Landau levels (CF-LLs), and exhibit the integer QHE. This picture has been very successful in obtaining excellent wave functions⁵. In the past few years, the experimental reality of CFs has also been firmly established⁶.

Great progress has also been made in arriving at a functional integral description in which some of the non-trivial properties found in the wave-function approach arise at the mean field level. The functional treatment is based on the Chern-Simons (CS) transformation⁷, which performs flux attachment via the CS gauge field to obtain either bosons⁸⁻¹¹ or fermions¹². These theories have provided us with a link between the microscopic formulation of the problem and experiment, both for incompressible and compressible states^{13,14}.

Recently R. Shankar and the present author developed a hamiltonian CS theory for the FQH states^{15,16}. Inspired by the work of Bohm and Pines¹⁷ on the 3D electron gas, we enlarged the Hilbert space to introduce n high-energy magnetoplasmons degrees of freedom, (n also being the number of electrons) at the same time imposing an equal number of constraints on physical states. Upon ignoring the coupling between the oscillators and the fermions we obtained some well known wavefunctions^{2,4}.

However the fermions still had the bare mass, and the frequency of the magnetoplasmons was incorrect. Hence a final canonical transformation was employed to decouple the fermions from the oscillators *in the infrared limit*.

We choose to call the final fermions *the composite fermions* for the following reasons. Firstly, the final fermions have no dispersion in the absence of interactions and acquire an effective mass dependent on interactions alone. Next, the final canonical transformation assigns to each fermion the magnetic moment $e/2m$ as mandated by the arguments of Refs.^{18,19}. The central result of our formalism is the formula for the electronic charge density, which takes the following form, separable into high- and low-energy pieces¹⁶, at small q :

$$\rho_e(q) = \frac{q}{\sqrt{8\pi}} \sqrt{\frac{2p}{2p+1}} (A(q) + A^\dagger(-q)) + \frac{\sum_j e^{-iqx_j}}{2p+1} - il^2 \left(\sum_j (q \times \Pi_j) e^{-iqx_j} \right) \quad (1)$$

where A, A^\dagger refer to the annihilation and creation operators of the magnetoplasmon oscillators, $l = 1/\sqrt{eB}$ is the magnetic length, and $\vec{\Pi}_j = \vec{P}_j + e\vec{A}^*(r_j)$ is the velocity operator of the CFs. The oscillator piece saturates Kohn's theorem²¹. The rest, to be called $\bar{\rho}$, is obtained by adding to the canonically transformed electronic charge density a particular multiple of the constraint¹⁶ (in the physical subspace, one can add any multiple of the constraint without physical consequences, but we wish to work in the full space). It has some very useful properties in the full space:

- $\bar{\rho}$ satisfies the magnetic translation algebra (MTA)²² to lowest leading order. Since this is the algebra of the electron density in the lowest Landau level (LLL), we have performed the LLL projection correctly in the infrared.
- Note that $\bar{\rho}$ is a sum of a monopole with charge $e^* = e/(2p+1)$, which is the charge associated with

the CF, and a dipole piece which alone survives at $\nu = 1/2$ and has the value proposed by Read²⁰. (A number of recent constructions have emphasized this dipolar aspect^{23–25}).

- We also find that as $\vec{q} \rightarrow 0$ all transition matrix elements of $\bar{\rho}$ from the HF ground state vanish at least as q^2 .

The final property is an essential property of *physical* charge density matrix elements from incompressible liquid ground states in the LLL²². We will present arguments in the next section to show that if one intends to use the Hartree-Fock approximation ignoring constraints, these properties of $\bar{\rho}$ are essential. They make it plausible that $\bar{\rho}$ does not suffer vertex corrections.

The Hamiltonian of the low-energy sector (dropping the magnetic moment term) is

$$H = \frac{1}{2} \int \frac{d^2q}{(2\pi)^2} v(q) \bar{\rho}(-q) \bar{\rho}(q). \quad (2)$$

where $v(q)$ is the electron-electron interaction. We circumvent the fact that $\bar{\rho}$ is to be trusted only for small q as follows. Consider real samples which have a finite thickness Λ of the same order as l , so that the Coulomb interaction is cutoff at large wavevectors²⁶. It was realized by Haldane and Rezayi²⁷ that this has a large effect on the gap, while leaving the wavefunctions essentially unchanged. We will focus on such interactions, parametrized by $\lambda = \Lambda/l$ for which numerical results for the transport gaps are available^{28–30}. The advantage is that as λ becomes large only small- q matrix elements of the density are invoked in computing gaps, and we expect our theory to become more accurate. It is possible that beyond some large λ the incompressible liquid might cease to be the ground state²⁷. Our theory, which is based on a liquid state with uniform density, can be expected to work up to this λ . In fact, the magnetoexciton dispersions can be used to infer these instabilities, as will be shown later.

This hamiltonian is to be supplemented by n constraints which identify the physical subspace. We will expand on this issue in the next section. In two earlier papers we presented calculations of gaps for a few fractions³¹ in the Hartree-Fock approximation, and tested certain scaling relations that arise naturally in the our theory against numerical results obtained using CF wave functions³². Emboldened by the good agreement we found between the predictions of our theory and numerical results, in this paper I present results for magnetoexciton (ME) dispersions for the polarized FQHE states at $\nu = \frac{1}{3}$, $\frac{2}{5}$, and $\frac{3}{7}$ based on our formalism. I will also present results for the spin-flip MEs, one branch (not always the lowest) of which corresponds to the spin waves in the ferromagnetic polarized states.

The computation of ME dispersions has a long history³³ in the IQHE. Many different approximations^{33,34} have been employed to obtain the ME dispersions in the IQHE, most of which can be subsumed into the powerful time-dependent HF (TDHF)

treatment of MacDonald^{35,36}. In this approach one allows the hamiltonian to scatter particle-hole excitations with different Landau-level indices into each other, and diagonalizes the resulting matrix.

A serious problem arises when considering ME dispersions in the FQHE. Since the states are strongly correlated in terms of electron variables, it is difficult to find good approximation techniques. Consequently, the most trusted results are those of exact diagonalizations on finite systems^{27,37}. There are also results from other methods, such as the single-mode approximation (SMA)²², which works well near the roton-like minimum for $\nu = \frac{1}{3}$, and the use of CF wavefunctions for excited states³⁸. Field-theoretic approaches include the seminal work of Lopez and Fradkin¹² for the collective modes of gapped fractions based on a fermionic CS approach, and an RPA treatment³⁹ based on the formalism of Halperin, Lee, and Read (HLR)¹⁴. These field-theoretic approaches suffer from the problem that the bare mass (actually the band mass m_b)¹² or a phenomenological mass m^* enters the dispersions, whereas in the LLL the scale should be set solely by $e^2/\epsilon l$.

Our approach essentially solves the problem of strong correlation by rewriting the theory in terms of CFs, which are the quasiparticles of the theory in the same sense as those in Landau's Fermi Liquid theory: The quasiparticles can interact strongly with a Fermi-Liquid-like interaction, but matrix elements which scatter them out of their states are small at low energies, allowing them to be long-lived. Furthermore, the only scale in our low-energy hamiltonian is indeed $e^2/\epsilon l$, as desired. For the reasons to be explained below, we *can* use a formalism such as TDHF, which ignores vertex corrections, with our formula for $\bar{\rho}$.

It must be emphasized that the TDHF approach of MacDonald^{35,36} which includes many Landau levels (LLs) is absolutely essential for treating the FQHE case. In the integer QHE one has two distinct energy scales, $\hbar\omega_c$ and $e^2/\epsilon l$, and one may go to the strong-field limit³⁴ $\hbar\omega_c \gg e^2/\epsilon l$ to make the problem theoretically convenient without losing any essential physics. In this limit only the lowest unoccupied and highest occupied LL need be considered, and LL-mixing of the MEs can be ignored. However, in our LLL analysis of the FQHE, there is only one energy scale, and the variation of energy within an ME mode is comparable to the splitting between different modes. We will see that the correct magnetoroton minimum cannot be obtained without considering this "CF-LL mixing".

The spin quantum number produces additional non-trivial features. It was realized by Sondhi *et al*⁴⁰ that even in the absence of Zeeman interactions, the $\nu = 1$ state, and correspondingly the Laughlin fractions $1/2p + 1$, were ferromagnetic due to exchange interactions. The symmetry-breaking leads to gapless spin waves with a quadratic dispersion. If the Zeeman interaction is now turned on the spin waves acquire a gap. Due to the fact that all other excitations of the system are much higher in energy than the spin waves, the $\nu = 1$ and the Laughlin fractions are dynamically identical to a simple quantum

ferromagnet at low temperatures⁴¹. The detailed predictions have been dramatically confirmed by experimental results⁴². There have been few attempts to compute the low-energy spin-flip modes for the polarized FQH states. One, due to Nakajima and Aoki⁴³, relates the FQH spin-wave mode to the IQH spin-wave mode, performing the flux-attachment by shifting the pseudopotentials. This, when tested against exact diagonalizations⁴³, produces good results for the $\nu = \frac{1}{3}$ and $\frac{1}{5}$ spin-wave modes. Another approach, by Mandal⁴⁴, uses fermionic CS theory to compute the response functions, and from them the spin-flip dispersions. In the spirit of the earlier CS approaches^{12,39} a phenomenological effective mass is used to approximate the energies of the CF-LLs, and the strong-field approximation is used. Where appropriate, we will comment on the relationship between these and our results.

The plan of the paper is as follows. In section II we will set up the conventions and define various terms. We will also show that the states with p filled CF-LLs are indeed HF ground states for $\nu = p/2p + 1$, and we will make some important remarks about the applicability of TDHF in our approximation scheme for the gapped fractions. In section III we describe the method of computing the ME dispersions, which is essentially MacDonald's approach³⁵ expressed in an operator form. In Section IV we present the results for the spin-polarized and the spin-flip ME dispersions and compare them to previous work. As mentioned earlier, beyond some Λ the incompressible FQHE state becomes unstable²⁷. Other instabilities include the transition to a Wigner crystal at small filling⁴⁵. The latter instability has been studied by looking at the ME dispersion in the $1/7$ ^{22,46} and $1/9$ systems⁴⁶. It is found that the ME dispersion becomes negative at finite wavevector⁴⁶ for the $1/9$ FQHE state, indicating that the ground state is unstable to the creation of large numbers of MEs. In analogy with this work, we will go back to the $\frac{1}{3}$, $\frac{2}{5}$, and $\frac{3}{7}$ FQHE states at large Λ and find instabilities in the ME dispersions for $\nu = \frac{2}{5}$ and $\frac{3}{7}$. We end with conclusions and open questions in section V.

II. SETTING UP THE FORMALISM

Let us return to the hamiltonian of equation (2), focussing for simplicity on spin-polarized states. Since we have a many-body Hamiltonian, we should choose a many-body ground state (GS). The formula for $\bar{\rho}$ contains the velocity operator for the CFs in the effective field $B^* = B/2p + 1$, suggesting that the CFs fill CF-LLs.

We now have a problem where the states are the same as those for (spinless) fermions in the IQHE. We work in the symmetric gauge, in which the single-particle wavefunctions are characterized by the LL index n and the angular momentum index k . The formalism in this gauge has been extensively developed^{2,47} in the context of anyon superconductivity. To conform to the notations of⁴⁷ we will define the magnetic field to be along the *pos-*

itive \hat{z} direction, which produces the wave functions

$$\phi_{n,k}(\vec{r}) = \frac{1}{\sqrt{2\pi 2^{n+k} n! k!}} \left(\frac{z}{2} - 2\partial^*\right)^n \left(\frac{z^*}{2} - 2\partial\right)^k e^{-|z|^2/4} \quad (3)$$

Here $z = x + iy$, and all distances are measured in units of the effective cyclotron length $l^* = l\sqrt{2p+1}$. Note that the LLL wave function is *antianalytic* with this choice of field direction.

The density is a one-body operator, and can create particle-hole pairs above the GS. It is well-known⁴⁸ that these pairs come with a conserved momentum \vec{q} , which also characterizes the separation between the particle and the hole $\vec{r}_{ph} = \hat{z} \times \vec{q} l^{*2}$. The magnetoexciton wave functions⁴⁸ $\psi_{nn'}(\vec{q}; \vec{r}, \vec{r}')$ describe a particle in the n^{th} LL and a hole in the n'^{th} LL. In the notation of ref.⁴⁷, it is expressed as

$$\psi_{nn'}(\vec{q}; \vec{r}, \vec{r}') = \frac{(-1)^n}{L} \frac{1}{\sqrt{2\pi 2^{n+n'} n! n'!}} (2\partial_1^* - \frac{z_1}{2})^n (2\partial_2 - \frac{z_2^*}{2})^{n'} e^{-\frac{1}{4}(r_1^2 + r_2^2 + Q^2)} e^{\frac{1}{2}(z_1^* z_2 + z_1 z_2^* - z_q^* z_2)} \quad (4)$$

Here L is the linear size of the system in units of l^* (the dimensionless area is L^2), and $z_q = iQ_+ = il^*(q_x + iq_y)$ is the dimensionless wavevector.

We can now define the x -coefficients, which denote the overlap between particular single-particle + single-hole states and the ME wavefunction as (for $k \geq k'$)

$$x_{nn'}^{kk'}(q) = \int d^2\vec{r}_1 d^2\vec{r}_2 \phi_{nk}^*(\vec{r}_1) \phi_{n'k'}(\vec{r}_2) \psi_{nn'}(\vec{q}; \vec{r}_1, \vec{r}_2) \\ = (-1)^{n'} \frac{\sqrt{2\pi}}{L} \sqrt{\frac{k!}{k'!}} \left(\frac{iQ_+}{\sqrt{2}}\right)^{k-k'} L_{k'-k}^{k'}(y) e^{-y/2} \quad (5)$$

Here L_n^m is a Laguerre polynomial, and $y = Q^2/2$. The x -coefficients are also the matrix elements of the unitary transformation that relates the product particle-hole basis with the ME basis. In order to obtain the x -coefficients for $k < k'$ we use

$$x_{n'n}^{k'k}(q) = (-1)^{n+n'} (x_{nn'}^{kk'}(-q))^* \quad (6)$$

Now we are ready to express $\bar{\rho}$ in this basis set. The form of $\bar{\rho}$ presented in Eq.(1) is correct for the field direction being $-\hat{z}$. In order to conform to the notation we are using⁴⁷ we have to use the following form

$$\bar{\rho}(q) = \frac{\sum_j e^{-iqx_j}}{2p+1} + il^2 \left(\sum_j (q \times \Pi_j) e^{-iqx_j}\right) \quad (7)$$

where Π_j is now the velocity operator in the effective field pointing in the $+\hat{z}$ direction. Now we invert Eq. (5) to get

$$\phi_{\nu_1}^*(\vec{r}_1) \phi_{\nu_2}(\vec{r}_2) = \int \frac{d^2q}{(2\pi)^2} (x_{\nu_2\nu_1}(q))^* \psi_{n_2n_1}(\vec{q}; \vec{r}_2, \vec{r}_1) \quad (8)$$

where we have used the compact notation $\nu_i = (n_i, k_i)$. To express the density in terms of second quantized operators we note that

$$\begin{aligned}\hat{\rho}(q) &= \int d^2r \left(\frac{e^{-iqr}}{2p+1} + il^2q \times \Pi e^{-iqr} \right) d^\dagger(\vec{r})d(\vec{r}) \\ &= \sum_{\nu_1\nu_2} \rho_{n_2n_1}(\vec{q})(x_{\nu_2\nu_1}(\vec{q}))^* d_{\nu_1}^\dagger d_{\nu_2}\end{aligned}\quad (9)$$

where we define

$$\begin{aligned}\rho_{n_2n_1}(\vec{q}) &= \int d^2r \psi_{n_2n_1}(q; \vec{r}, \vec{r}) \left(\frac{e^{-iqr}}{2p+1} + il^2q \times \Pi e^{-iqr} \right) \\ &= \frac{(-1)^{n_1}}{2p+1} \frac{L}{\sqrt{2\pi}} \sqrt{\frac{n_1!}{n_2!}} \left(\frac{-iQ_+}{\sqrt{2}} \right)^{n_2-n_1} \\ &\quad \times e^{-y/2} (n_2 L_{n_1-1}^{n_2-n_1} + 2L_{n_1}^{n_2-n_1} - (n_1+1)L_{n_1+1}^{n_2-n_1})\end{aligned}\quad (10)$$

This last expression is valid for $n_2 \geq n_1$. For $n_2 < n_1$ one uses the relation

$$\rho_{n_2n_1}(\vec{q}) = (-1)^{n_1+n_2} (\rho_{n_1n_2}(-\vec{q}))^* \quad (11)$$

In what follows, it will be useful to define the magnetoexciton operators

$$\hat{X}_{n_1n_2}(\vec{q}) = \sum_{k_1k_2} (x_{\nu_2\nu_1}(\vec{q}))^* d_{\nu_1}^\dagger d_{\nu_2} \quad (12)$$

where the sums are over the angular momentum indices. Finally, one can compactly express the electron density operator as

$$\hat{\rho}(\vec{q}) = \sum_{n_1n_2} \rho_{n_2n_1}(\vec{q}) \hat{X}_{n_1n_2}(\vec{q}) \quad (13)$$

Apart from the trivial dependence of x on n' , we see the separation between the angular k labels and the ‘‘radial’’ n labels.

We will need the following identities, which can be easily established by using the defining relation for x , Eq. (5);

$$\sum_k x_{nn}^{kk}(\vec{q}) = (-1)^n \frac{L}{\sqrt{2\pi}} \delta_{\vec{Q},0} \quad (14)$$

$$\begin{aligned}\sum_k x_{n_1n}^{k_1k}(\vec{q}_1) x_{n_2n}^{k_2k}(\vec{q}_2) &= (-1)^n \frac{\sqrt{2\pi}}{L} e^{\frac{-i}{2}\vec{Q}_1 \times \vec{Q}_2} \times \\ &\quad x_{n_1n_2}^{k_1k_2}(\vec{q}_1 + \vec{q}_2)\end{aligned}\quad (15)$$

A. Calculation of Gaps

As mentioned before, we have to assume a many-body ground state. Since the low-energy hamiltonian contains the velocity operator in the effective field $B^* = B/2p+1$, it is natural to assume a ground state of p filled CF-LLs for $\nu = p/2p+1$. This is not an eigenstate of H , which can create particle-hole pairs above it. However, it is the HF ground state. We now establish that, for rotationally invariant interactions, the Hamiltonian does not mix a single-particle (or single-hole) state with any other single-particle (or single-hole) state. This is the signature of a HF state.

We begin by writing down the hamiltonian in terms of the CF creation and annihilation operators

$$\begin{aligned}H &= \int \frac{d^2q}{(2\pi)^2} \frac{v(q)}{2} \sum_{\nu_i} x_{\nu_4\nu_1}^*(-\vec{q}) x_{\nu_3\nu_2}^*(\vec{q}) \\ &\quad \times \rho_{n_4n_1}(-\vec{q}) \rho_{n_3n_2}(\vec{q}) d_{\nu_1}^\dagger d_{\nu_4} d_{\nu_2}^\dagger d_{\nu_3}\end{aligned}\quad (16)$$

Consider the transition matrix element of H between two *different* single-particle states $\mu = (m, k) \neq (m', k') = \mu'$ on top of the assumed GS of p filled CF-LLs;

$$\begin{aligned}\langle GS | d_\mu H d_{\mu'}^\dagger | GS \rangle &= \frac{1}{2} \int \frac{d^2q}{(2\pi)^2} v(q) \sum_{\nu_i} \\ &\quad \rho_{n_4n_1}(-\vec{q}) \rho_{n_3n_2}(\vec{q}) x_{\nu_4\nu_1}^*(-\vec{q}) x_{\nu_3\nu_2}^*(\vec{q}) \\ &\quad \langle GS | d_\mu d_{\nu_1}^\dagger d_{\nu_4} d_{\nu_2}^\dagger d_{\nu_3} d_{\mu'}^\dagger | GS \rangle\end{aligned}\quad (17)$$

Now we perform the usual Wick contractions (at equal time) with

$$\langle GS | d_\nu^\dagger d_{\nu'} | GS \rangle = \delta_{\nu\nu'} N_F(\nu) \quad (18)$$

$$\langle GS | d_\nu d_{\nu'}^\dagger | GS \rangle = \delta_{\nu\nu'} (1 - N_F(\nu)) \quad (19)$$

where $N_F(\nu)$ denotes the occupation of the single-particle state ν . In performing the Wick contractions one should take care not to contract the two operators belonging to the same density (say $d_{\nu_1}^\dagger$ with d_{ν_4}), since this leads to the $\vec{q} = 0$ density, which is cancelled by the background positive charge. Now we can write the transition matrix element as

$$\begin{aligned}(1 - N_F(\mu))(1 - N_F(\mu')) \int \frac{d^2q}{(2\pi)^2} \frac{v(q)}{2} \sum_{\nu} \left(\right. \\ \left. (1 - N_F(\nu)) x_{\nu\mu}^*(-\vec{q}) x_{\mu'\nu}^*(\vec{q}) \rho_{nm}(-\vec{q}) \rho_{m'n}(\vec{q}) - \right. \\ \left. N_F(\nu) x_{\mu'\nu}^*(-\vec{q}) x_{\nu\mu}^*(\vec{q}) \rho_{m'n}(-\vec{q}) \rho_{nm}(\vec{q}) \right)\end{aligned}\quad (20)$$

We now use the x -identities to perform the sum over the angular momentum index of ν in the two terms to get a factor of $x_{\mu\mu'}^*(\vec{q}=0)$ in both terms. The explicit form of x tells us that setting $\vec{q} = 0$ forces $k = k'$. This leaves the integral over the reduced density matrix elements. Consider the first term for specificity

$$H_1 = \frac{\pi \delta_{kk'}}{L^2} \int \frac{d^2q}{(2\pi)^2} v(q) \sum_{n \geq p} (-1)^{m+n} \rho_{mn}(-q) \rho_{nm'}(q) \quad (21)$$

By using the explicit functional form of the density matrix elements, Eqs. (10) and (11), we can reduce this to the form

$$H_1 = \frac{\pi \delta_{kk'}}{L^2} \int \frac{d^2q}{(2\pi)^2} v(q) \sum_{n \geq p} f(m, m', n, q^2) e^{i\theta(m-m')} \quad (22)$$

where θ is the angle of \vec{q} with respect to the q_x axis. It is then clear that for $m \neq m'$, the rotational invariance

of $v(q)$ will force this term to be zero. The same result can be verified for the second term, and also for the case of two different single-hole states.

This establishes the HF nature of the GS, and supports our view that we are working with the right variables. We can now verify from Eq. (10), as claimed in the introduction, that as $\vec{q} \rightarrow 0$ all transition matrix elements from the HF ground state vanish at least as q^2 , an essential property of charge density matrix elements in the LLL²².

Let us now find the energy of a single-particle state above the filled sea. This is just the diagonal matrix element of H , and we have already done most of the work. Setting $m = m'$ in the above, we get

$$\epsilon(m) = \frac{\pi}{L^2} \int \frac{d^2q}{(2\pi)^2} v(q) \sum_n (1 - 2N_F(n)) |\rho_{nm}(\vec{q})|^2 \quad (23)$$

The first term is the Hartree energy while the second represents the exchange, or Fock part. The hamiltonian can be normal ordered to make this obvious in operator form

$$H = H_0 + V$$

$$H_0 = \sum_{\nu} \epsilon_0(n) d_{\nu}^{\dagger} d_{\nu} \quad (24)$$

$$V = \int \frac{d^2q}{(2\pi)^2} \frac{v(q)}{2} \sum_{\nu_i} x_{\nu_4\nu_1}^* (-\vec{q}) x_{\nu_3\nu_2}^* (\vec{q})$$

$$\times \rho_{n_4n_1}(-\vec{q}) \rho_{n_3n_2}(\vec{q}) d_{\nu_1}^{\dagger} d_{\nu_2}^{\dagger} d_{\nu_3} d_{\nu_4} \quad (25)$$

$$\epsilon_0(n) = \frac{\pi}{L^2} \int \frac{d^2q}{(2\pi)^2} v(q) \sum_n |\rho_{nm}(\vec{q})|^2 \quad (26)$$

Similarly, one can easily derive the hole energy, which is identical to the above, except for a minus sign. Notice that the energies depend only on the CF-LL index, and not on the angular momentum, and that there is a sum over an infinite tower of CF-LLs in the energy.

So far our discussion is applicable to arbitrary $v(q)$. Below we will find it convenient to specialize to a model potential that approximates the effects of sample thickness $v(r) = e^2/\epsilon\sqrt{r^2 + \Lambda^2}$, whose Fourier transform is $v(q) = 2\pi e^2 \exp(-q\Lambda)/\epsilon q$. The parameter Λ is related to the sample thickness.

At this point, two important questions arise: We have treated the hamiltonian in the HF approximation, and we have ignored constraints altogether. It is important to understand whether these approximations are reasonable, and how they might (at least in principle) be improved. The next four subsections will address these issues in turn.

B. Why is Hartree-Fock reasonable?

Hartree-Fock is an approach that works best when correlations are weak. The ground state is sought to be expressed in terms of a single determinant of single-particle wave functions. Clearly, carrying out a HF calculation in terms of *electron* coordinates would be nonsensical in the FQHE problem: This is the message that Laughlin's work² has driven home. However, what we are doing here

is radically different. We are working in terms of CF coordinates. The correlated ground state of electrons can be viewed as the ground state of independent CFs, which is the message of Jain's work⁵. In other words, the system of electrons reorganizes itself into a state where the CFs are the Fermi-liquid-like quasiparticles. Thus one can reasonably expect to get good results from a simple approximation such as HF when working in CF coordinates.

However, one other condition has to be satisfied if the results are to be numerically accurate. We have to make sure that vertex corrections are small. Large vertex corrections imply that the particle we started out with is not the physically observed quasiparticle, *i.e.*, that the observed charge, dipole moment, etc are different from those entering the microscopic hamiltonian. In this case, the HF excited states will have small overlap with the true excited states, and the HF energies will be correspondingly poor. Our formula for $\bar{\rho}$ does have the correct charge and dipole moments of the final physical particles. In other words, they are already fully dressed, and therefore vertex corrections are expected to be small.

There is another way to conclude that vertex corrections are small for $\bar{\rho}$: Recall¹⁶ that in order to get $\bar{\rho}$ we took a particular multiple of the constraint and added it to the "naive" transformed electron density. In principle, one can add any multiple of the constraint to the density, and the physical matrix elements should be unaffected. However, this particular combination has a very nice property which we have mentioned before: All its transition matrix elements from the HF ground state are order q^2 or higher. This is a necessary property of all *physical* density matrix elements in the incompressible fractions²². This property does not hold for the naive transformed density, or for any other linear combination of the density and the constraint; they all have transition matrix elements of order q from the assumed HF ground state. Of course, if the constraint were exactly implemented, it would force all physical matrix elements to behave correctly by producing vertex corrections. Thus, every combination except our $\bar{\rho}$ is *guaranteed* to suffer strong vertex corrections. Therefore we come to an important conclusion: If we intend to use HF without implementing the constraint exactly, we must use $\bar{\rho}$, and only $\bar{\rho}$, for the electron density operator.

C. Constraints

Since it is very hard to implement these constraints exactly, we will use two different approaches. The first approach is to ignore the constraints altogether. The rationale for doing this is the following: Suppose we had the exact expression for the electron density operator in final coordinates. Since this operator is gauge invariant (*i.e.* commutes with the constraints), it will have no matrix elements between the true physical ground state and unphysical states. Thus the sum over physical states can be extended to a sum over all states with no problem. However, this requires that we also have the correct physical

ground state. In practice we have neither an exact expression for ρ_e nor the true ground state. However, our $\bar{\rho}$ is close to an operator that is gauge invariant⁴⁹ (we will elucidate this in subsection E), and we can hope that the ground state we choose is close to the true one, so that all the above statements are approximately correct.

While this approach indeed produces reasonable answers for the thickness parameter $\lambda \geq 2.0$ or so, it produces an unphysical divergence of the transport gap for $\lambda = 0$ ³¹. The reason is not far to seek. For small λ the potential has significant weight at large q , where our expression for $\bar{\rho}$ is not to be trusted. Thus in this region, our $\bar{\rho}$ couples to unphysical states, of which there are an infinite number, which produces the divergence. Thus, in order to get a physically sensible answer for small λ one is forced to account for the constraint in some way. We choose the simplest possible way, by cutting off the high energy CF-LL states. There are many ways of seeing that such a cutoff makes physical sense. Firstly, for a finite number of particles, there are a finite number of states in the many-body Hilbert space (after projecting to the LLL, which we do by freezing oscillators), equivalent in dimensionality to the Hilbert space generated by $2p + 1$ CF-LLs. Secondly, density matrix elements in the LLL are suppressed at high momenta by gaussian factors. Matrix-elements of our $\bar{\rho}$ between higher CF-LL states are peaked at higher momenta, and thus it is plausible that the higher CF-LLs are less physical. Finally, even in the LLL, we expect CFs to describe only the low-energy dynamics. At energies of the order of the first Haldane pseudopotential⁵⁰ V_1 , we expect the CF to break up into electrons and vortices. Thus, CF-LLs cannot be the correct description at high energies. On the other hand, there is ample numerical evidence that the low-lying CF-LLs are very close to true physical states⁵¹.

Thus we have the following picture: The higher CF-LLs probably have very little overlap with physical states, while the lower ones have large overlap. This argument does not tell us precisely which states we must keep. In the rest of this paper I will choose a sharp cutoff in the CF-LLs, wherein some number (around $2p + 1$) of the lowest ones are kept, and the rest discarded. We will also investigate how sensitive our results are to a change in this cutoff, and we will find that for $\lambda \geq 2.0$ or so, the results become insensitive, and that one can keep all the CF-LLs without much altering the results. The main operational aim of this method of implementing the constraints is to obtain qualitatively reasonable (though perhaps numerically untrustworthy) results for small λ .

Thus far we have given arguments mostly from within our theory. Of course, the correct way to settle matters of principle is to implement the constraints from the start on an equal footing with the hamiltonian. Such a calculation has not been carried out for the gapped fractions, but Read²⁵ has recently studied the case of $\nu = 1$ bosons in detail (this belongs to class of compressible systems, among which is included the half-filled LLL for electrons^{13,14}), where constraints are crucial in restoring compressibility to the system^{14,23,25,52,53}. We devote the next subsection to the lessons we can draw from Read's

work²⁵.

D. Read's Conserving Approximation for $\nu = 1$ Bosons

Read²⁵ starts from the LLL formulation of Pasquier and Haldane²⁴ for $\nu = 1$ bosons, and implements the constraints (which, unlike the constraints in our formulation^{15,16}, do not commute among themselves, but form an algebra) in a path-integral conserving approximation⁵⁴. Our greatest interest is in the gaps and ME dispersions, which can be read off as the poles of the density-density correlator. Let us therefore focus on his results for the irreducible density correlator χ_{irr} , for which he finds²⁵ that:

- χ_{irr} breaks up naturally into two additive contributions. The first is the density correlator of dipoles, while the second represents the dipoles interacting with a transverse gauge field. It should be emphasized that the fermions that enter the lagrangian have charge e , and that a nontrivial renormalization has happened due to vertex corrections in order to make them dipolar.
- The contribution due to the transverse gauge field dominates at very low frequency, restoring compressibility to the system. This contribution controls the ω^0 and the ω^{-1} moments of the density spectral function.
- At higher frequencies, the purely dipolar part dominates. For example, the ω moment of the density spectral function is identical to the result for purely dipolar fermions.

Let us view our method in the light of these results. Our fermionic density, written in terms of $\bar{\rho}$, is dipolar (for $\nu = \frac{1}{2}$) already at tree level, and no further vertex corrections are necessary. What is missing in our approach is the coupling to the low-energy transverse gauge field. However, this contribution seems to be relatively unimportant at high frequencies.

While we are not certain how all this might extend to the gapped fractions, we can make the following plausible guesses: The vertex corrections will renormalize the charge of the fermion from e to e^* , and produce a dipole moment (and perhaps higher multipole moments). Once again this renormalization (upto dipole terms) is present in our $\bar{\rho}$ already at tree level. Secondly, we can expect a gauge field to enter the picture. However, we once again expect it to be important only at low frequencies. Since all the answers we seek in the gapped fractions are at finite frequencies of the order of the gaps, we do not expect the gauge field to make a large contribution to our results.

To summarize, the effects of the constraint in Read's calculation are twofold: They renormalize the charge and dipole moment, and they create a transverse gauge field to which the dipolar fermions are coupled, and which is

important at low frequencies. The first effect is present in full in our approach, while we argue that for the physical quantities of interest to us, the contribution of the second can be safely ignored in the gapped fractions.

We now turn to a very recent new formulation for the gapped fractions.

E. Shankar's New Formulation for Principal Fractions

Very recently, Shankar⁴⁹ has proposed formulas for the charge density and constraint for all principal fractions. He writes both the electronic charge density (call it $\bar{\rho}_S$) and the constraint (call it χ_S) as a sum over exponentials of single-CF coordinates. The first two terms of each exponential are exactly the two terms derived in our earlier work¹⁶. $\bar{\rho}_S$ and χ_S have some very nice properties:

- $\bar{\rho}_S$ satisfies the MTA *to all orders* in q . This formulation is not restricted to the infrared.
- χ_S also satisfies the MTA with a modified magnetic length, and is identified as the vortex charge density⁴⁹. (It should be noted that this is different from our original formulation, since our constraints commute^{15,16}, and should continue to do so after the canonical transformations).
- $\bar{\rho}_S$ and χ_S commute with each other, so $\bar{\rho}_S$ is gauge invariant.
- The hamiltonian can be written in terms of $\bar{\rho}_S$, which makes it gauge invariant, and amenable to a conserving approximation.

Such a conserving approximation would be the way to settle matters of principle, such as the quantum numbers of the excitations in the gapped fractions, and their statistics³. However, Shankar also points out⁴⁹ that there is another possible formulation of the problem that is very closely related to that followed in this paper, and provides a justification of it. He notes that one can form a preferred charge density

$$\bar{\rho}_{pref} = \bar{\rho}_S + c\chi_S \quad (27)$$

where c is the charge of the vortex. This charge density has a very appealing physical interpretation, since each composite fermion has an electron and a vortex in close proximity, and $\bar{\rho}_{pref}$ is just the total charge of such a composite. One can now express the hamiltonian in terms of $\bar{\rho}_{pref}$, and it commutes weakly with the constraints ($[H, \chi] \simeq \chi$). In the physical subspace this is as good a formulation as the one in the previous paragraph.

Most important for our purposes, the first two terms of this preferred charge density are exactly the two terms in our $\bar{\rho}$, Eq. (1). Therefore $\bar{\rho}_{pref}$ enjoys all the nice properties of $\bar{\rho}$, such as explicitly displaying the right charge and dipole moment, satisfying the MTA at lowest leading order, and having q^2 matrix elements out of the HF ground

state. Shankar points out⁴⁹ that if one is interested in computing numbers in the gapped fractions, this second formulation, with many nontrivial renormalizations built in at tree level, may produce better numbers than the conserving approach.

This second viewpoint meshes perfectly with our philosophy. It also gives us an algebraically consistent way to continue the expression for $\bar{\rho}$ to all orders in q . When one looks at the corrections to our $\bar{\rho}$ by comparing it to Shankar's $\bar{\rho}_{pref}$, one finds that the leading order correction (order q^2) vanishes, and the next correction (order q^3) is down by a large factor (≈ 500)⁴⁹. This suggests that while our $\bar{\rho}$ was derived at small q , its regime of validity may be larger than we have any right to expect.

To summarize the past four subsections, we have presented several lines of reasoning that suggest that by using our $\bar{\rho}$ for the electronic charge density, we are working in a preferred representation where the effect of constraints is minimal, and approximations such as HF and TDHF can be expected to give good answers. We now proceed to the calculations.

III. METHOD OF CALCULATION

Conventionally, in using the TDHF approximation³⁵, one first computes the density matrix under a time-dependent perturbation, and thence the behavior of the density with time to linear order in the external potential. The susceptibility is directly connected to the density-density correlator, and its poles give the ME dispersions.

We will be following an operator variant of this method, where we will directly determine the time dependence of the ME operators (defined in Eq. (12)) by commuting them with the hamiltonian. This method also has an ancient history⁵⁵. The expression on the right hand side will, in the spirit of HF, be simplified by reducing four-fermi operators to two-fermi ones by taking averages.

We will initially consider the simpler spin-polarized case, and later show how to extend the formalism to include spin.

A. Spin-Polarized Magnetoexcitons

For a Heisenberg operator we have the relation

$$\frac{\partial O}{\partial t} = i[H, O] \quad (28)$$

Let us begin by considering the time dependence of the ME operator $\hat{X}_{m_1 m_2}(q)$ by computing $[\hat{H}, \hat{X}_{m_1 m_2}(q)]$. We will find it convenient to use the form of \hat{H} split into Hartree and interaction terms as given in Eqs. (24,25). It is then easy to verify that

$$[\hat{H}_0, \hat{X}_{m_1 m_2}(\vec{q})] = (\epsilon_0(m_1) - \epsilon_0(m_2))\hat{X}_{m_1 m_2}(\vec{q}) \quad (29)$$

where ϵ_0 is just the Hartree energy of Eq. (26). To compute the next term we will need

$$\begin{aligned} & [d_{\nu_1}^\dagger d_{\nu_2}^\dagger d_{\nu_3} d_{\nu_4}, d_{\mu_1}^\dagger d_{\mu_2}] = \\ & \delta_{\mu_1\nu_4} d_{\nu_1}^\dagger d_{\nu_2}^\dagger d_{\nu_3} d_{\mu_2} - \delta_{\mu_2\nu_1} d_{\mu_1}^\dagger d_{\nu_2}^\dagger d_{\nu_3} d_{\nu_4} \\ & - \delta_{\mu_1\nu_3} d_{\nu_1}^\dagger d_{\nu_2}^\dagger d_{\nu_4} d_{\mu_2} + \delta_{\mu_2\nu_2} d_{\mu_1}^\dagger d_{\nu_1}^\dagger d_{\nu_3} d_{\nu_4} \end{aligned} \quad (30)$$

The hamiltonian has the symmetry $(\nu_1, \nu_3) \rightarrow (\nu_2, \nu_4)$, and hence in the following we will keep only the first two terms (Eq. (30)), while removing the factor of $\frac{1}{2}$ in front of the interaction. Also, in TDHF one has to reduce all the four-point to two-point terms. We do this by contracting one creation and one annihilation operator in all possible ways, remembering that the operators that belong to the same density are not allowed to contract together (such a term would correspond to a uniform density, which is cancelled by the positive background). These terms can be grouped as follows:

$$N_F(m_1) \delta_{\mu_2\nu_1} (\delta_{\mu_1\nu_3} d_{\nu_2}^\dagger d_{\nu_4} - \delta_{\mu_1\nu_4} d_{\nu_2}^\dagger d_{\nu_3}) \quad (32)$$

$$+ N_F(m_2) \delta_{\mu_1\nu_4} (\delta_{\nu_1\mu_2} d_{\nu_2}^\dagger d_{\nu_3} - \delta_{\nu_2\mu_2} d_{\nu_1}^\dagger d_{\nu_3}) \quad (33)$$

$$+ N_F(n_2) \delta_{\mu_2\nu_1} \delta_{\nu_2\nu_4} d_{\mu_1}^\dagger d_{\nu_3} - N_F(n_1) \delta_{\mu_1\nu_4} \delta_{\nu_1\nu_3} d_{\nu_2}^\dagger d_{\mu_2} \quad (34)$$

Now we multiply the above by the appropriate factors and integrate over \vec{q} , and use the x -identities. It is easy to show that the last line (Eq. (34)) produces just the Fock energies of m_1, m_2 , which occur in the right combination to add to $[\hat{H}_0, \hat{X}]$ to give

$$(\epsilon(m_1) - \epsilon(m_2)) \hat{X}_{m_1 m_2}(\vec{q}) \quad (35)$$

Let us now consider the more interesting terms from Eq. (32) and Eq. (33). There are four such terms, and they are equal in pairs. Performing the Wick contractions and using the identities (bearing in mind that $\delta_{\vec{Q},0} = \frac{(2\pi)^2}{L^2} \delta^2(\vec{Q}) = \frac{(2\pi)^2}{L^2(l^*)^2} \delta^2(\vec{q})$), we obtain

$$\begin{aligned} [\hat{V}, X_{m_1 m_2}(\vec{q})] = & - \sum_{n_1 n_2} X_{n_1 n_2}(\vec{q}) (N_F(m_1) - N_F(m_2)) \times \\ & \left((-1)^{m_1+m_2} \frac{1}{(l^*)^2 L^2} v(q) \rho_{m_1 m_2}(-\vec{q}) \rho_{n_2 n_1}(\vec{q}) \right. \\ & \left. - (-1)^{m_1+m_2} \frac{2\pi}{L^2} \int \frac{d^2 s}{(2\pi)^2} v(s) \rho_{m_1 n_1}(-\vec{s}) \rho_{n_2 m_2}(\vec{s}) e^{i\vec{s} \times \vec{Q}} \right) \end{aligned} \quad (36)$$

where $\vec{Q} = l^* \vec{q}$, $\vec{S} = l^* \vec{s}$. For the case of the diagonal matrix elements, *i.e.*, $(n_1 n_2) = (m_1 m_2)$, these two terms have a simple physical meaning. The first term is the direct interaction between the particles, which shows up as an *exchange* interaction between the particle and the hole, while the second is the exchange interaction between particles, or the *direct* Coulomb interaction between the particle and hole. We can now write the entire commutator as

$$\begin{aligned} [\hat{H}, \hat{X}_{m_1 m_2}(\vec{q})] = & (\epsilon(m_1) - \epsilon(m_2)) \hat{X}_{m_1 m_2}(\vec{q}) \\ & - (N_F(m_1) - N_F(m_2)) \sum_{n_1 n_2} (-1)^{m_1+m_2} \hat{X}_{n_1 n_2}(\vec{q}) \times \end{aligned}$$

$$\begin{aligned} & \left(\frac{v(q)}{L^2 l^{*2}} \rho_{m_1 m_2}(-\vec{q}) \rho_{n_2 n_1}(\vec{q}) \right. \\ & \left. - \int \frac{d^2 s}{(2\pi)^2} v(s) e^{i\vec{s} \times \vec{Q}} \frac{2\pi}{L^2} \rho_{m_1 n_1}(-\vec{s}) \rho_{n_2 m_2}(\vec{s}) \right) \end{aligned} \quad (38)$$

The hamiltonian can now be thought of as a matrix in the space of “naive” MEs, which are represented by the \hat{X} operators. These are not eigenoperators of \hat{H} , which has transition matrix elements between different naive MEs. An important point is that both positive and negative energy naive MEs are connected by the hamiltonian, which is not hermitian. Nevertheless, the eigenvalues will occur in pairs $\pm\omega_j$, with $\omega_j \geq 0$ being identified as the energy of a ME mode. Finally, notice that both terms of an arbitrary transition matrix element go to zero in the limit of large q , the first because the matrix elements $\rho_{nn'}$ are suppressed with gaussian factors, and the second due to the oscillatory factor $e^{i\vec{Q} \times \vec{S}}$. Thus the naive MEs decouple and become the eigenstates of the TDHF hamiltonian in the limit of large q .

The density matrix elements $\rho_{n_1 n_2}$ are complex, which means that generic Hamiltonian matrix elements are also complex. To simplify the future discussion we define the following *reduced density matrix element* $\tilde{\rho}$ by the defining relation

$$\rho_{n_1 n_2}(\vec{q}) = \frac{L}{\sqrt{2\pi}} \frac{1}{(2p+1)} e^{i(n_1 - n_2)(\theta_q - \pi/2)} \tilde{\rho}_{n_1 n_2}(Q) \quad (39)$$

where $\tilde{\rho}$ is real, symmetric in $n_1 n_2$, independent of the direction of \vec{q} , and is a function of $Q = l^* q$ alone. It is clear that the $\tilde{\rho}$ matrix element can be made real by choosing $\theta_q = \pi/2$, thus making the direct matrix element of H , Eq. (36), real. The same choice also makes the exchange matrix element, Eq. (37), real. The fact that all matrix elements of H in the ME subspace are real speeds the numerical diagonalization.

B. Scaling of ME Dispersions

The discussion so far is valid for an arbitrary potential. Let us now specialize to our model potential

$$v(q) = \frac{2\pi e^2}{q} e^{-\Lambda q} = \frac{2\pi l^* e^2}{Q} e^{-\lambda^* Q} \quad (40)$$

where $\lambda^* = \Lambda/l^*$. Using the definition of the Bessel function

$$J_n(z) = \int_{-\pi}^{\pi} \frac{d\theta}{2\pi} e^{iz \sin \theta - in\theta} \quad (41)$$

and fixing $\theta_q = \pi/2$, we can perform the angular integration and cast the direct and exchange matrix elements into the form (ignoring the factor of $-(N_F(m_1) - N_F(m_2))$)

$$V_d(m_1 m_2 : n_1 n_2) = K_p \frac{\tilde{\rho}_{n_1 n_2}(Q) \tilde{\rho}_{n_3 n_4}(Q)}{Q} e^{\lambda^* Q} \quad (42)$$

$$V_x(m_1 m_2 : n_1 n_2) = -K_p (-1)^{n_1 + m_2} \times$$

$$\int_0^\infty dS e^{-\lambda^* S} \tilde{\rho}_{m_1 n_1}(S) \tilde{\rho}_{n_2 m_2}(S) J_{m_1 - m_2 + n_2 - n_1}(QS) \quad (43)$$

Here $K_p = \frac{e^2}{t_0(2p+1)^{5/2}}$ is a common energy scale. It turns out that the factor K_p can also be extracted from the HF energies to get

$$e(m) = \frac{\epsilon(m)}{K_p} = \frac{1}{2} \int_0^\infty dS \sum_n |\tilde{\rho}_{nm}(S)|^2 (1 - 2N_F(n)) \quad (44)$$

Since the overall factor of K_p can be extracted from the entire TDHF hamiltonian, it follows that the ME dispersions scale with K_p . Now suppose we had analyzed the fraction $\nu(p, r) = p/(2pr + 1)$. Everything above would have followed unchanged except for the replacement $2p+1 \rightarrow 2pr+1$, and hence K_p and λ^* would change, but nothing else (it is important to note that the ground state still consists of p filled CF-LLs). Thus, in our approach, the ME dispersions at the same p , but different r , are related by scaling. This is an extension of the scaling relations for gaps that we verified in an earlier publication³². This scaling holds exactly in our theory provided the constraints are ignored. If the constraints are taken into account by cutting off the CF-LLs, then of course a r dependence will creep into the ME dispersions.

C. Spectral Function and Spectral Weight

It is frequently of interest to determine how much of the spectral weight is being carried by various modes, and in particular, the lowest mode. Such considerations are crucial for the success of the single mode approximation (SMA)²², which is known to be good near the roton minimum for $\frac{1}{3}$. Let us go back to the TDHF hamiltonian of Eq.(38), and assume that we have diagonalized it into modes α

$$H_{m_1 m_2 : n_1 n_2}^{TDHF}(\vec{q}) \Psi_{n_1 n_2}^{R\alpha}(\vec{q}) = E_\alpha(\vec{q}) \Psi_{m_1 m_2}^{R\alpha}(\vec{q}) \quad (45)$$

$$\Psi_{n_1 n_2}^{L\alpha}(\vec{q}) H_{n_1 n_2 : m_1 m_2}^{TDHF}(\vec{q}) = E_\alpha(\vec{q}) \Psi_{m_1 m_2}^{L\alpha}(\vec{q}) \quad (46)$$

where the sum over $n_1 n_2$ is implicit. Note that since H^{TDHF} is not hermitian we need to consider both right and left eigenvectors.

Now we can go back and add an external time-dependent potential $V(\vec{q}, \omega) e^{-i\omega t}$ that couples to the electron density in the hamiltonian. It is easy to verify that the equation for the response of the magnetoexciton operators to the external potential is

$$(\omega \delta_{m_1 m_2 : n_1 n_2} + H_{m_1 m_2 : n_1 n_2}^{TDHF}) \bar{X}_{n_1 n_2}(\vec{q}, \omega) = (N_F(m_1) - N_F(m_2)) \frac{V(\vec{q}, \omega)}{l^* 2 L^2} \rho_{m_2 m_1}(\vec{q}) \quad (47)$$

We can resolve any function of H^{TDHF} in terms of its eigenvectors and eigenvalues, and in particular, we can invert the above equation to obtain

$$\bar{X}_{m_1 m_2}(\vec{q}, \omega) = \sum_{\alpha : n_1 n_2} \Psi_{m_1 m_2}^{R\alpha}(\vec{q}) \frac{1}{\omega + E_\alpha} \Psi_{n_1 n_2}^{L\alpha}(\vec{q}) \times \frac{(N_F(n_1) - N_F(n_2))}{l^* 2 L^2} \rho_{n_2 n_1}(\vec{q}) V(\vec{q}, \omega) \quad (48)$$

Recalling the expansion of the density in terms of the magnetoexciton operators, Eq.(13), we obtain for the density response

$$\langle \bar{\rho} \rangle = \sum_{\alpha : m_1 m_2 n_1 n_2} \rho_{m_2 m_1}(\vec{q}) \Psi_{m_1 m_2}^{R\alpha}(\vec{q}) \frac{1}{\omega + E_\alpha} \Psi_{n_1 n_2}^{L\alpha}(\vec{q}) \times \frac{(N_F(n_1) - N_F(n_2))}{l^* 2 L^2} \rho_{n_2 n_1}(\vec{q}) V(\vec{q}, \omega) \quad (49)$$

Now we use the fact that due to the peculiar structure of H^{TDHF} for spin-polarized MEs $\Psi_{m_1 m_2}^{L\alpha} = (N_F(m_1) - N_F(m_2)) \Psi_{m_1 m_2}^{R\alpha}$. Further, using the definition of the reduced density matrix elements, Eq. (39), we obtain the susceptibility to be

$$\chi(\vec{q}, \omega) = \sum_{\alpha} \frac{A_\alpha}{\omega + E_\alpha} \quad (50)$$

where

$$A_\alpha = \frac{\left(\sum_{m_1 m_2} \tilde{\rho}_{m_2 m_1}(\vec{q}) \Psi_{m_1 m_2}^{R\alpha}(\vec{q}) \right)^2}{2\pi(2p+1)^2 l^{*2}} \quad (51)$$

In the TDHF approximation all the modes are sharp, and do not decay. The spectral function is then a sequence of delta functions at the energies $\pm E_\alpha$ with weight A_α . Of course, if we go beyond TDHF, all the modes except the lowest will acquire a finite width. Even the lowest mode may have a dispersion which kinematically permits a quantum of high q to decay into two or more quanta of lower q .

To summarize, our approach to computing the spin-polarized ME dispersions will be to compute the TDHF hamiltonian matrix in the subspace of MEs, and to diagonalize it. If constraints are ignored, this subspace is infinite-dimensional, since there is an infinite tower of CF-LLs. We will follow the usual prescription of increasing the number of CF-LLs kept till the answer converges. For small λ we find that the gap is unphysically large, and diverges as $\lambda \rightarrow 0$. Here we will follow the discussion presented earlier and keep a finite number of CF-LLs, approximately equal to $2p + 1$, to get a qualitative idea of the predictions of our theory in this regime. It should be emphasized that we trust the results only for $\lambda \geq 1.5$ or so. Fortunately, this seems to be close to the physical regime for high-density samples^{30,56}.

Let us now turn to the spin-flip MEs.

D. Spin-Flip Magnetoexcitons

In order to incorporate the spin quantum number we must go back to the beginning and ask how the flux attachment is accomplished in the initial representation.

As implicit in the early wave-function formulation of Halperin⁶⁰, and pointed out explicitly by Lopez and Fradkin⁶¹, there are many inequivalent ways to attach flux, where particles with like spin see each other as carrying $2r_1$ units of statistical flux, while those with unlike spin see each other as carrying $2r_2$ units. We will work in the picture where the number of flux units seen by other particles is independent of the spin, and will deal with the case of $r_1 = r_2 = 1$ for simplicity. For this case, the statistical gauge field remains a scalar in the spin indices, and still satisfies

$$\nabla \times \vec{a}(\vec{r}) = 4\pi\rho(\vec{r}) \quad (52)$$

The sequence of canonical transformations^{15,16} goes through exactly as before, and we arrive at the final representation of the electron density projected to the low-energy subspace, expressed in second quantized form as

$$\hat{\rho}(\vec{q}) = \sum_{\sigma, n_1 n_2} \rho_{n_2 n_1}(\vec{q}) \hat{X}_{\sigma, n_1 n_2}(\vec{q}) \quad (53)$$

where we define the spin- σ ME operators

$$\hat{X}_{\sigma, n_1 n_2}(\vec{q}) = \sum_{k_1 k_2} (x_{\nu_2 \nu_1}(\vec{q}))^* d_{\sigma, \nu_1}^\dagger d_{\sigma, \nu_2} \quad (54)$$

In other words the total density is the sum of the \uparrow and \downarrow charge densities. One can also define the spin-density operators projected to the low-energy subspace

$$\hat{S}_z(\vec{q}) = \sum_{\sigma, k_1 k_2} (x_{\nu_2 \nu_1}(\vec{q}))^* \rho_{n_2 n_1}(\vec{q}) \frac{\sigma}{2} d_{\sigma, \nu_1}^\dagger d_{\sigma, \nu_2} \quad (55)$$

$$\hat{S}_+(\vec{q}) = \sum_{k_1 k_2} (x_{\nu_2 \nu_1}(\vec{q}))^* \rho_{n_2 n_1}(\vec{q}) d_{\uparrow, \nu_1}^\dagger d_{\downarrow, \nu_2} \quad (56)$$

$$\hat{S}_-(\vec{q}) = \sum_{k_1 k_2} (x_{\nu_2 \nu_1}(\vec{q}))^* \rho_{n_2 n_1}(\vec{q}) d_{\downarrow, \nu_1}^\dagger d_{\uparrow, \nu_2} \quad (57)$$

The projected spin and charge operators no longer commute with each other, unlike the full spin and charge operators. Instead they form a representation (to lowest leading order in q) of the LLL spin-charge algebra discussed previously in ref.⁵⁹. For our purposes, it is useful to define the spin-flip ME operators

$$\hat{Y}_{+, n_1 n_2}(\vec{q}) = \sum_{k_1 k_2} (x_{\nu_2 \nu_1}(\vec{q}))^* d_{\uparrow, \nu_1}^\dagger d_{\downarrow, \nu_2} \quad (58)$$

$$\hat{Y}_{-, n_1 n_2}(\vec{q}) = \sum_{k_1 k_2} (x_{\nu_2 \nu_1}(\vec{q}))^* d_{\downarrow, \nu_1}^\dagger d_{\uparrow, \nu_2} \quad (59)$$

We will be dealing exclusively with fully polarized states for simplicity, though the method can be trivially extended to partially polarized states as well. Let us arbitrarily designate \uparrow as the sign of the majority spin. There will be an additional Zeeman energy of $E_Z(n_\downarrow - n_\uparrow)/2$. Since the hamiltonian commutes with the z -component of the total spin, this energy can be added to the spin-flip excitations at the end. We will therefore ignore the Zeeman term when computing the dynamics. As in the previous subsection, we commute the hamiltonian with \hat{Y}_\pm and find the hamiltonian matrix in the subspace of spin-flip MEs. The final result is

$$\begin{aligned} [\hat{H}, \hat{Y}_{-, m_1 m_2}(\vec{q})] &= (\epsilon_\downarrow(m_1) - \epsilon_\uparrow(m_2)) \hat{Y}_{-, m_1 m_2}(\vec{q}) \\ &- (N_{F\downarrow}(m_1) - N_{F\uparrow}(m_2)) \sum_{n_1 n_2} \hat{Y}_{-, n_1 n_2}(\vec{q}) V_x(m_1 m_2; n_1 n_2) \end{aligned} \quad (60)$$

where V_x is the same exchange matrix element as in Eq. (43). We also define the spin-dependent HF energies as

$$\epsilon_\sigma(m) = \frac{\pi}{L^2} \int \frac{d^2 q}{(2\pi)^2} v(q) \sum_n (1 - 2N_{F\sigma}(n)) |\rho_{nm}(\vec{q})|^2 \quad (61)$$

where $N_{F\sigma}(m)$ denotes the spin-dependent Fermi occupation of the single-particle state m . Note that only modes which have $(N_{F\downarrow}(m_1) - N_{F\uparrow}(m_2)) \neq 0$ need be considered. In the fully polarized states $N_{F\downarrow}(m) = 0$ for all m , and this restricts us to consider $N_{F\uparrow}(m) = 1$. The ‘‘negative energy’’ MEs appearing in the previous subsection are absent here, and the TDHF hamiltonian matrix is hermitian.

Let us briefly note that the formalism developed in this section can be directly applied to the very interesting case of double-layer quantum Hall systems, which have been the subject of much recent interest^{62,63}.

We are now ready to present the results.

IV. RESULTS

A. Gaps

In a previous publication Shankar and the present author have presented results for the transport gap in a few fractions³¹, calculated using the methods of section II. We pause here to view the gaps in a slightly different light. In many field-theoretic approaches to computing the ME dispersions it is assumed that the interactions produce CF-LLs whose energy dependence on the CF-LL index n is cyclotron-like

$$E_n = n\omega_c^* \quad (62)$$

Indeed, in the CS approach of Lopez and Fradkin¹², this is the exact result in lowest order, with the bare mass m setting the scale for ω_c^* . This seems to be a natural assumption. On the other hand, in the LLL, all splittings are the result of interactions, and there is no *a priori* reason why they should follow Eq. (62). In our approach we can compute these energies, and can therefore test this hypothesis. In Table 1 we present the energies of the CF-LLs for $\nu = \frac{1}{3}$, for $n_{max} = 5$. We have set the energy of the $n = 0$ CF-LL to 0, and normalized all energies in units of $E_{n=1}$. The cyclotronic prediction for this normalization is $E_n = n$.

λ	E_1	E_2	E_3	E_4	E_5
0.0	1.00	1.75	2.37	2.88	3.32
1.0	1.00	1.48	1.76	1.90	1.89
2.0	1.00	1.32	1.50	1.54	1.43
3.0	1.00	1.22	1.35	1.38	1.27

It is quite clear that there are strong deviations from the cyclotronic form. These deviations become greater as the sample thickness increases. In particular, for $\lambda \geq 1.0$ we find the strange result that E_5 is less than E_4 . This is another manifestation of the unphysical nature of the higher CF-LLs. For higher λ there is a distinct tendency for the energies to fall towards E_1 , to form almost a continuum above E_1 . All these features are present for the other fractions as well.

To emphasize the collective nature of the energies, we present the spin-dependent HF energies in the absence of Zeeman interactions for $\nu = \frac{2}{5}$ at $\lambda = 1.0$, with $n_{max} = 4$ in Table II.

n	0	1	2	3	4
$E_{n\uparrow}/K_2$	-0.36	0.81	2.62	3.39	3.40
$E_{n\downarrow}/K_2$	2.35	3.74	4.68	5.20	5.07

Here K_2 is an example of the constant K_p defined in Section III B. The majority (\uparrow -spin) and minority (\downarrow -spin) energies are quite different for the same CF-LL index, even when the Zeeman coupling is zero, because the majority spin energy has a large negative exchange contribution, while the minority spin energy has only a Hartree contribution. Neither of the energies has a cyclotronic form.

We therefore come to the conclusion that the cyclotronic form of the energy should be regarded with skepticism.

B. Spin-Polarized Magnetoexcitons

Figure 1 shows the ME dispersions for $\nu = \frac{1}{3}$, at a $\lambda = \Lambda/l_0 = 1.5$. We are using a cutoff on the number of CF-LL's, n_{max} , denoted by "nx" in the figure. The solid line denotes the "naive" ME. In other words, we take the state created by the ME operator $\hat{X}_{10}(\vec{q})$ and just compute its energy as a function of q . The energy of the naive ME corresponds to the strong-field limit for the IQHE. It is clear that including the other ME's, and the interaction between them, drastically alters the dispersion. In particular, the magnetoroton minimum present in the other dispersions is missing in the naive one. We conclude that the strong-field limit is not justified in the FQHE.

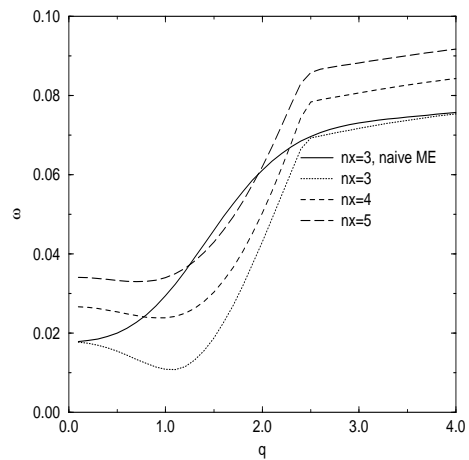


FIG. 1. Spin-polarized ME dispersions for $\nu = 1/3$ at $\lambda = 1.5$ for different values of n_{max} . All energies are in units of $e^2/\epsilon l$. The solid line is the energy of the "naive" ME, which corresponds to the strong-field limit in the IQHE.

Let us now turn to the evolution of the dispersions with q and n_{max} . As q increases the energy asymptotically tends to the transport gap, which itself increases with n_{max} . The gap at $n_{max} = 5$ is about half its value for $n_{max} = \infty$. However, the gap at $n_{max} = 5$ is about 20% *greater* than the true gap³⁰ for $\lambda = 1.5$.

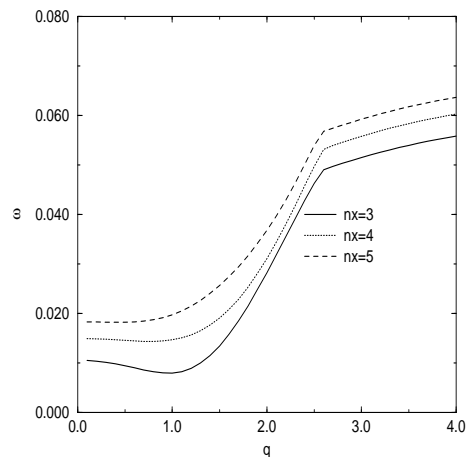


FIG. 2. Spin-polarized ME dispersions for $\nu = 1/3$ at $\lambda = 2.0$ for different values of n_{max} .

The roton minimum is very shallow and the value of the energy at $q = 0$ is quite small. The q at the minimum is about $1.1l_0^{-1}$, slightly smaller than the corresponding value for the pure Coulomb interaction. This is qualitatively consistent with the results of the SMA²². However, for $q = 0$ the quasiparticle and the quasihole are right on top of each other, and our charge density operator may not have enough short distance structure to get the right numbers for small λ . For large λ , however, the potential becomes very flat at short distances, and we expect better results.

Fig. 2 shows the same picture for $\lambda = 2.0$. As can be seen, the fractional change in the transport gap as n_{max}

increases is even smaller here (the $n_{max} = \infty$ value of the gap is now about 50% higher than that for $n_{max} = 5$, which is itself 20% higher than the true gap³⁰). The magnetoroton minimum is even smaller and seems to shift slightly towards smaller q .

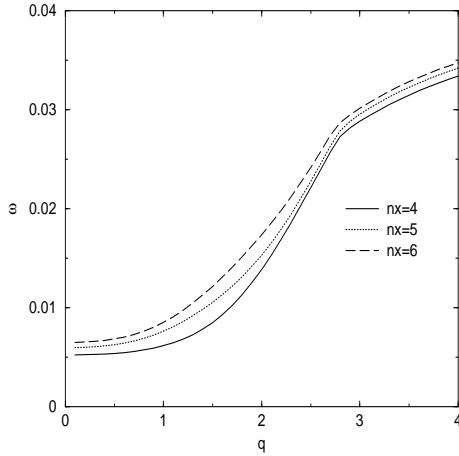


FIG. 3. Spin-polarized ME dispersions for $\nu = 1/3$ at $\lambda = 3.0$ for different values of n_{max} .

To continue the trend towards greater thickness we show the corresponding results for $\lambda = 3.0$ in Fig. 3, for which the $n_{max} = \infty$ value of the gap is 35% higher than that for $n_{max} = 5$, which is itself within 10% of the true gap. The minimum at finite ql has disappeared and the minimum is now at $q = 0$.

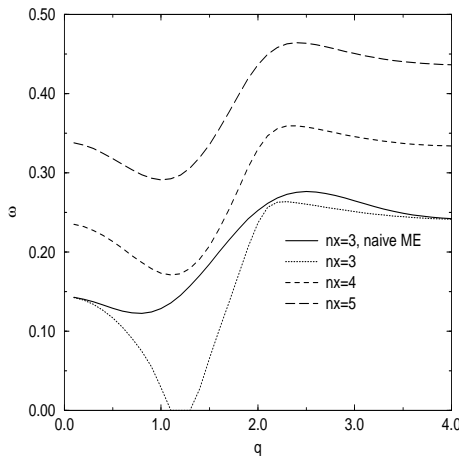


FIG. 4. Spin-Polarized ME dispersions for $\nu = 1/3$ at $\lambda = 0.0$ for different values of n_{max} . Note that the dispersion shows an instability for $n_{max} = 3$, but none for $n_{max} > 3$.

Fig. 4 shows the same calculation done for the pure Coulomb interaction, $\lambda = 0.0$. For $n_{max} = 3$ one finds that the dispersion becomes unstable for a range of q between $1.1l_0^{-1}$ to $1.35l_0^{-1}$. However, the instability disappears if n_{max} is increased, and now there is a deep magnetoroton minimum around $ql_0 = 1.25$, which is the correct position^{27,22,37,38}. However, the values of the energy are much larger than the true values. Thus, while

a qualitatively correct picture is obtained for $n_{max} \geq 4$, we cannot trust the numbers for the Coulomb interaction. The main reason is probably because, as pointed out above, our $\bar{\rho}$ misses the short-distance physics which is important for the Coulomb interaction.

Since our approach is a dynamical theory of CFs, we can obtain all the ME dispersions for a given n_{max} . To emphasize this, Fig. 5 shows all the ME dispersions for $\nu = \frac{1}{3}$, $\lambda = 2.0$, and $n_{max} = 4$.

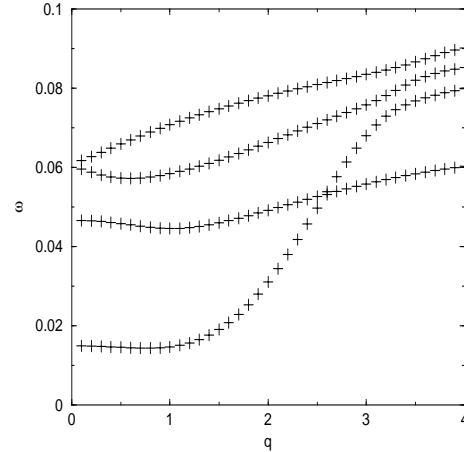


FIG. 5. All the ME dispersions for $\nu = 1/3$ at $\lambda = 2.0$ for $n_{max} = 4$. The lowest mode is well-separated but the others form a quasi-continuum.

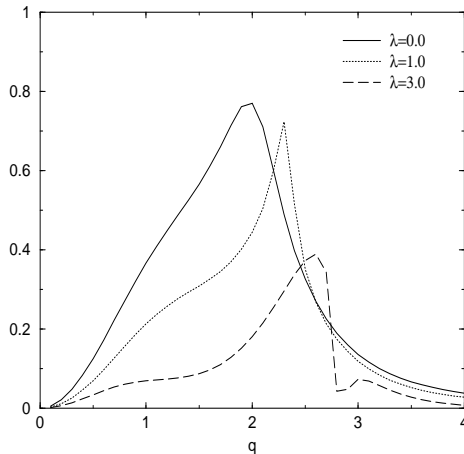


FIG. 6. Fraction of spectral weight carried by the lowest mode for $\nu = 1/3$ at $n_{max} = 4$ for different values of λ . Note that the lowest mode carries vanishing spectral weight for large and small q , and that its spectral weight decreases drastically with increasing λ .

In Fig. 6 we show the fraction of total spectral weight in the lowest mode for different values of λ . The value of n_{max} has been set at 4 for all the curves. Two features stand out: Firstly, the lowest mode carries vanishing spectral weight at small and large q , regardless of λ . This means that the SMA will overestimate the gap for $q = 0$ and for large q . Secondly, it is clear that for small

λ , much of the spectral weight is in the lowest mode for intermediate values of ql . These two facts are known for $\lambda = 0.0$ from exact diagonalizations⁵⁰. Our calculation actually underestimates the weight for $\lambda = 0.0$ (which, to the author's knowledge, is the only case where it has been previously computed). However, our results also show that the lowest mode carries a decreasing fraction of the spectral weight with increasing λ , which means that the SMA will become less useful for larger λ .

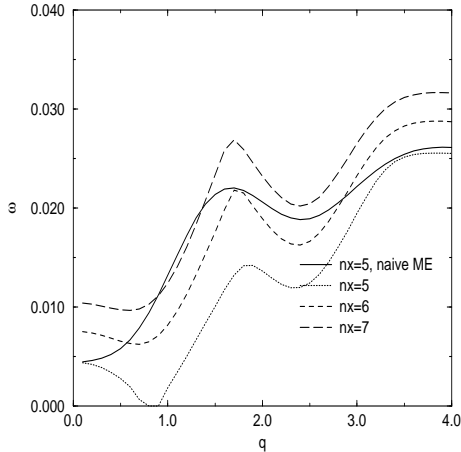


FIG. 7. Spin-polarized ME dispersions for $\nu = \frac{2}{5}$ at $\lambda = 1.5$ for different values of n_{max} .

The next set of five figures presents results of similar calculations for $\nu = \frac{2}{5}$. Here $n_{max} = 5$ shows instabilities for $\lambda = 1.5, 2.0$, while $n_{max} \geq 6$ shows the right behavior (we will comment in detail on instabilities in the next subsection). The minima appear at $ql_0 = 0.85, 2.4$.

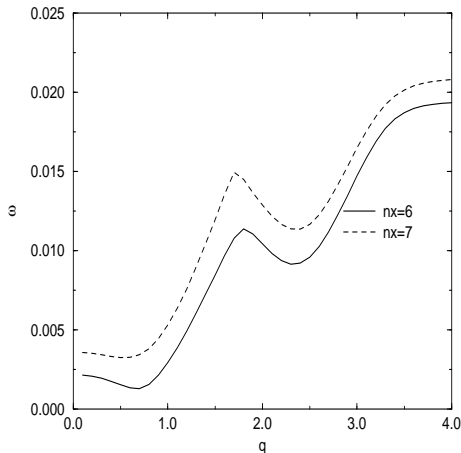


FIG. 8. Spin-polarized ME dispersions for $\nu = \frac{2}{5}$ at $\lambda = 2.0$ for different values of n_{max} .

While the position of the first minimum is consistent with the results of exact diagonalizations, the second minimum seems to be too high in q (exact diagonalizations³⁷ and other^{38,39} numerical results indicate the second minimum at $ql_0 = 1.6$).

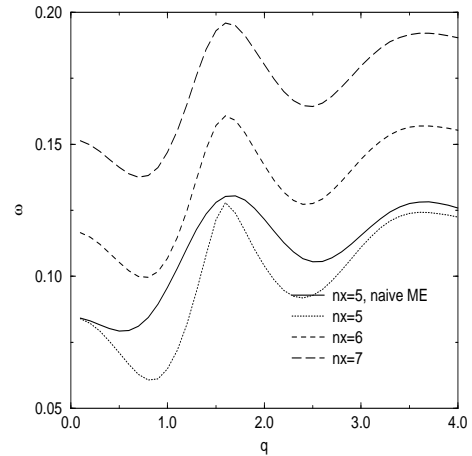


FIG. 9. Spin-polarized ME dispersions for $\nu = \frac{2}{5}$ at $\lambda = 0.0$ for different values of n_{max} .

Fig. (10) shows all the dispersions for $\lambda = 2.0$ and $n_{max} = 8$. It is clear that beyond the lowest ME mode, there is almost a continuum of excitations (recall that these are by no means all the excitations; these are only the single quasiparticle-single quasihole excitations).

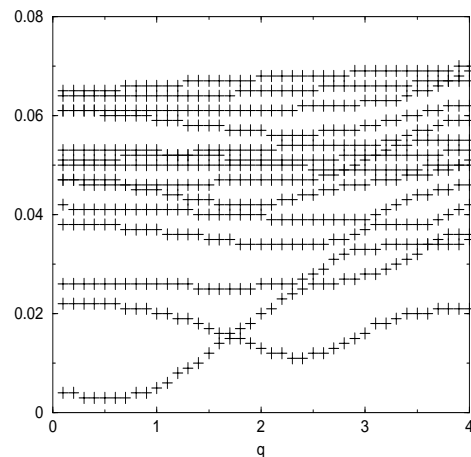


FIG. 10. All the ME dispersions for $\nu = \frac{2}{5}$ at $\lambda = 2.0$ for $n_{max} = 8$. The lowest mode is well-separated but the others form a quasi-continuum.

In Fig. 11 we present the fraction of the spectral weight in the lowest mode for $n_{max} = 7$. It is clear that this is lower for all q at $\lambda = 0.0$ than in the case of $\frac{1}{3}$. Once again, as λ increases the fraction of the spectral weight in the lowest mode decreases.

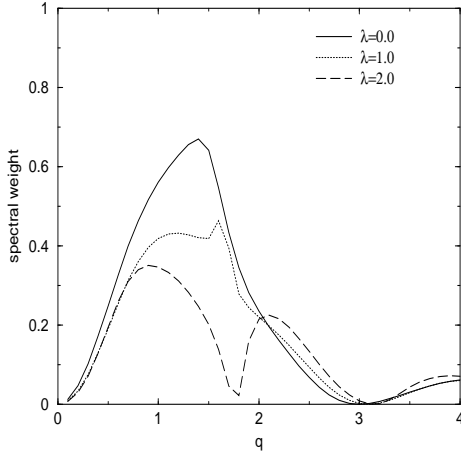


FIG. 11. Fraction of spectral weight carried by the lowest mode for $\nu = \frac{2}{5}$ at $n_{max} = 7$ for different values of λ . Just as in the $\nu = \frac{1}{3}$ case the lowest mode carries vanishing spectral weight for large and small q , and its spectral weight decreases with increasing λ .

Finally, we turn to $\nu = \frac{3}{7}$, for which we present results for $n_{max} = 10$ only, and for values of $\lambda = 0.0, 1.0, 2.0$. We find that the position of first minimum agrees with that from exact diagonalizations³⁷ and CF-wavefunction calculations³⁸ ($ql \approx 0.6$), while the second and third minima seem to be displaced to higher q , just as in the $\nu = \frac{2}{5}$ case.

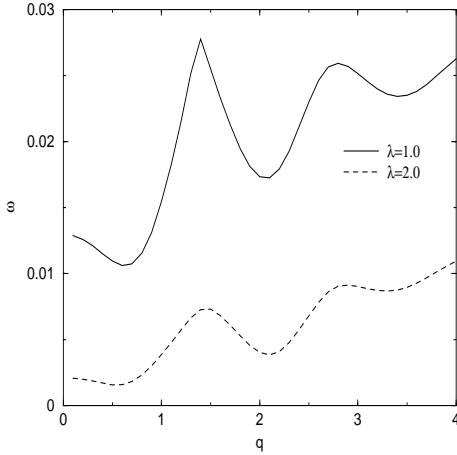


FIG. 12. Spin-polarized ME dispersions for $\nu = \frac{3}{7}$ at $\lambda = 1.0$ and 2.0 for $n_{max} = 10$.

Fig. 14 shows the spectral weight in the lowest mode, which looks very similar to the $\frac{2}{5}$ case. We do not really trust our results quantitatively for small λ . Therefore, while one can definitely say that for all fractions the spectral weight decreases as thickness increases, it is difficult to see any other clear trend (such as a trend with increasing denominator).

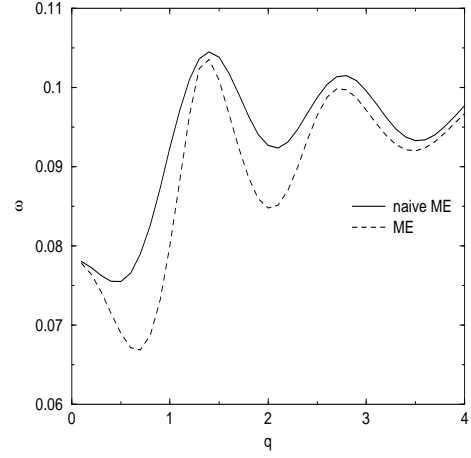


FIG. 13. Spin-polarized ME dispersions for $\nu = \frac{3}{7}$ at $\lambda = 0.0$ for $n_{max} = 10$.

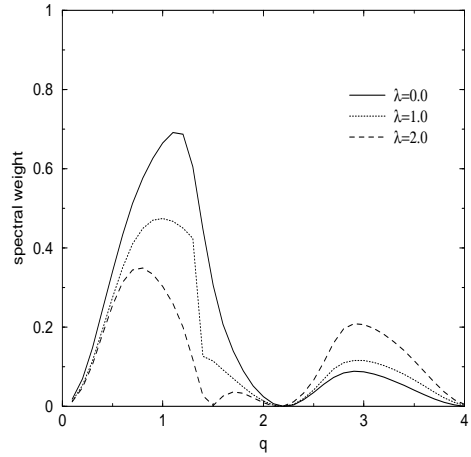


FIG. 14. Fraction of spectral weight carried by the lowest mode for $\nu = \frac{3}{7}$ at $n_{max} = 10$ for different values of λ . Just as in the $\nu = \frac{1}{3}$ case the lowest mode carries vanishing spectral weight for large and small q , and its spectral weight decreases with increasing λ .

In conclusion, our results with a cutoff on n_{max} appear to be in qualitative agreement with numerical results for $\lambda = 0$. However, there are quantitative discrepancies which make them unreliable for small λ . The reasons for the failure of our theory to reproduce numbers at small λ are well-understood, and have been repeatedly mentioned above.

On the other hand, we expect our theory to be quantitatively good at large λ . Recall that for $2.0 \leq \lambda \leq 3.0$ our results³¹ for the transport gap were within 30% of the numerical values³⁰. What needs to be done is to compare our results to numerical ones at large λ . Unfortunately, exact diagonalizations and other numerical methods have so far concentrated on the pure Coulomb interaction, and few results on ME dispersions are available for large λ . In the absence of exact results, our results are predictions for the ME dispersions.

We now turn to a brief discussion of instabilities.

C. Instabilities Inferred from Magnetoexciton Dispersions

The use of ME dispersions to study instabilities was pioneered by Girvin, MacDonald, and Platzman in their seminal paper on the SMA²². While they did not find actual instances where the ME dispersion became negative, they did find that for $\nu = 1/7$, the magnetoroton minimum nearly touched zero. On this basis, they conjectured that in the presence of disorder, the gaps would be reduced, and since the potential instability is at finite wavevector, that there would be a quantum phase transition to a Wigner crystal⁴⁵. Kamilla and Jain⁴⁶ have demonstrated within the CF-wavefunction approach that for $\nu = 1/9$ for the pure Coulomb interaction, the ME dispersion indeed becomes negative at a finite wavevector, signalling an instability of the incompressible liquid. The transition is expected to be first order, and probably occurs before (*i.e.* for ν greater than the ν for which) the ME dispersion becomes negative.

Our interest will be in instabilities as a function of the thickness parameter λ . While one can always make a CF variable by fiat, by attaching two statistical flux quanta to an electron, the experimental reality of the CF depends on energetics. It is helpful to think of the case of $\nu = \frac{1}{3}$ in terms of the Haldane pseudopotentials V_m ⁵⁰. These pseudopotentials give the energy of a pair of electrons in the LLL with relative angular momentum m . The Laughlin state has no pairs in a relative $m = 1$ state. The reason this is such a good trial state for the Coulomb potential is that V_1 is much bigger than V_3 , and there are no other states without pairs in $m = 1$. This is also why the state is incompressible: Every excitation must necessarily have an amplitude for creating a pair in an $m = 1$ state, and costs a large energy of order V_1 . Now let us make the sample thicker. As λ increases the ratio V_3/V_1 increases, and at some critical value of this ratio, the system will make a transition to a compressible state²⁷. This transition is expected to be first order²⁷, but one may still look for signals of this transition in the incompressible state.

In this spirit, I have analyzed the ME dispersions as a function of both λ and n_{max} . First consider the $\nu = 1/3$ state. I find that while there appear to be instabilities at finite q for small n_{max} (an example is Fig. 4), they disappear when one increases n_{max} . So I find no reliable signs of instability for $\nu = \frac{1}{3}$. However, for $\nu = \frac{2}{5}$, I find that at $\lambda_{cr} = 2.65$ the ME dispersion becomes zero at $ql \approx 0.4$. I have increased n_{max} to 10 (much larger than the rough cutoff of $2p + 1 = 5$ from section), and observed that the instability persists. Similarly, I find that for $\nu = \frac{3}{7}$, there is a finite wavevector instability at $\lambda_{cr} = 2.4$. It is interesting that the λ_{cr} is not the same for for fractions which share the same number of flux attached, but decreases with increasing denominator.

Experimentally, such instabilities would be seen as the lack of a fractionally quantized plateau beyond a certain sample density, even at zero temperature. Presumably, the above numbers for λ_{cr} are overestimates for the ex-

perimental values of the thickness parameter, since disorder, which has not been taken into account here, will further reduce the gaps.

Let us now turn to the spin-flip ME dispersions.

D. Spin-Flip Magnetoexcitons

Figure 15 shows our results for $\nu = \frac{1}{3}$ for the pure Coulomb interaction in the absence of a Zeeman term. What is shown is the lowest branch, which corresponds in this case to the spin-wave mode. In accordance with Goldstone's theorem, the energy vanishes as $q \rightarrow 0$ (quadratically, as it should for a ferromagnet). Upto about $ql_0 \approx 1$ the dispersion for $n_{max} = 3$ agrees quite well with the exact diagonalization results of Nakajima and Aoki⁴³, and thus also gives approximately the correct spin stiffness.

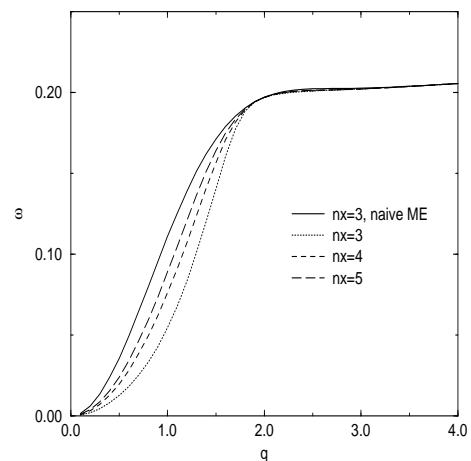


FIG. 15. Spin-wave dispersion for $\nu = \frac{1}{3}$ at $\lambda = 0.0$ for different values of n_{max} . As n_{max} increases the separation between levels increases, decreasing the interaction between naive MEs.

Once again, the “naive” spin-flip ME is higher in energy than the true mode by almost a factor of two in this region, and interaction between the various naive modes results in closer agreement with exact results. In this context the accuracy of the results of Nakajima and Aoki⁴³ based on flux attachment appear puzzling, since the strong-field limit is implicit in their approach. On the other hand, $\lambda = 0.0$ is the worst case for our theory, and perhaps it is our agreement with the spin-wave energy that is more surprising. It is difficult to compare our results to Mandal's work⁴⁴, since in the spirit of earlier work in the fermionic CS approach^{12,39} a phenomenological effective mass appears, and the cyclotronic hypothesis is used for the energies.

As $q \rightarrow \infty$ the ME energy tends asymptotically to the spin-reversed gap (which is considerably overestimated by our theory at $\lambda = 0.0$). It is important to note that all higher spin-flip modes are well separated from the lowest one for small q , which justifies identifying the low-

energy dynamics of the polarized $\frac{1}{3}$ state with that of the quantum ferromagnet⁴¹.

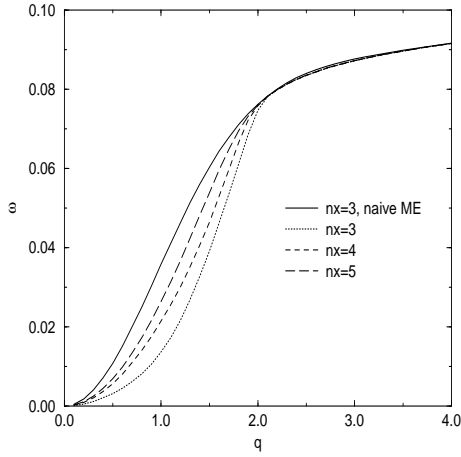


FIG. 16. Spin-wave dispersion for $\nu = \frac{1}{3}$ at $\lambda = 1.0$ for different values of n_{max} .

We follow the progression as λ increases in Fig. 16. Once again, it is unfortunate that numerical results are not available for large λ , where we expect our theory to be quantitatively accurate. Note, that for the spin-reversed gap, our prediction is about 30% higher the exact answer²⁹ for λ as low as 1.5.

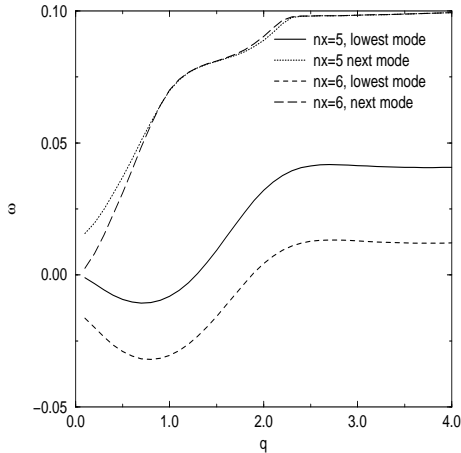


FIG. 17. Lowest and next lowest spin-flip modes for $\nu = \frac{2}{5}$ at $\lambda = 0.0$ for different values of n_{max} . Note that the energy of the lowest mode is negative for a substantial range of q , and that there is a roton-like minimum.

Next we present the spin-flip excitations for $\frac{2}{5}$, and here there is a new feature. While there is always a gapless quadratically dispersing mode, it is not always the lowest mode. For $n_{max} = 5$ the gapless mode has negative energy for small q , while for $n_{max} = 6$, the gapless mode has positive energy, but the negative energy mode persists, and becomes gapped. The lowest mode at large q is one which takes an up-spin particle from the $n = 1$ CF-LL and replaces it as a down-spin particle in the $n = 0$ CF-LL. At large q the energy of this excita-

tion is positive, making the spin-reversed gap positive. However, as shown in Figs. 17 and 18, there is always a negative energy mode at small q . In the absence of a Zeeman coupling this implies an instability of the polarized ground state. It is known from previous work⁶⁴ comparing ground state energies that the spin-singlet $\frac{2}{5}$ state is lower in energy than the spin-polarized state for small E_Z . The zero-temperature transition between the states is expected to be first order, but nonetheless, one can look for signatures of the instability in the polarized state.

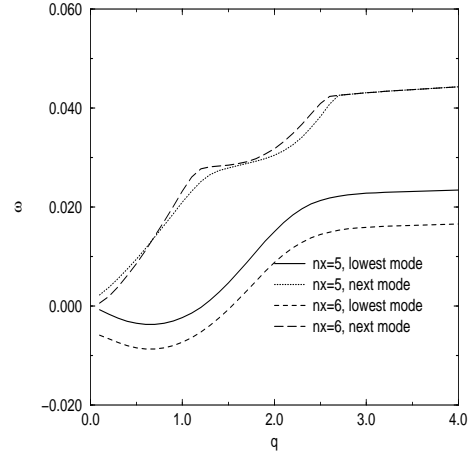


FIG. 18. Lowest and next lowest spin-flip modes for $\nu = \frac{2}{5}$ at $\lambda = 1.0$. All the features observed for $\lambda = 0.0$ are present.

In fact, from Fig. 18 we can infer that at $\lambda = 1.0$ (presumably close to the physical range of sample thickness), the transition to the polarized state should take place when a uniform shift of the ME dispersion upwards by E_Z makes the dispersion always positive, *i.e.*, for $\frac{E_Z}{c^2/\epsilon l} \geq 0.01$. Experimentally⁶⁵, it is found that $E_Z \approx 0.015e^2/\epsilon l$.

In the presence of a Zeeman energy E_z capable of stabilizing a polarized ground state, our result implies that the lowest spin-flip mode will have a roton-like minimum at finite q , and that the smallest gap to excitations is lower than E_z . This in turn would indicate a much faster reduction of the magnetization with temperature than in the case of $\frac{1}{3}$, and a finite-temperature spin-structure factor peaked at nonzero momentum. Perhaps the most significant consequence of this result is that one can no longer think of the polarized $\frac{2}{5}$ state as a simple quantum ferromagnet.

V. CONCLUSIONS

I have used the dynamical theory of Composite Fermions developed by Shankar and myself^{15,16} to compute the magnetoexciton dispersions for a few gapped fractions. The TDHF method of MacDonald^{35,36} was

used to do these computations. Let me reiterate that this method is the minimal one in the present case since there is only one energy scale. My primary motivation is to see how far our theory can take us, and what its limitations are. To this end, the constraint was imposed in its crudest form, by cutting off the CF-LLs at n_{max} . Some such cutoff is certainly necessary on physical grounds, as explained in section II.

Our results for spin-polarized ME dispersions are in qualitative agreement with exact diagonalizations^{27,37}, and other numerical methods^{22,38}, for the pure Coulomb interaction ($\lambda = 0.0$). This is the worst case for our theory, since our expression for the charge density is valid at long wavelengths, and the Coulomb interaction has a significant short-distance part. As a consequence, there are significant numerical discrepancies for $\lambda = 0.0$.

On the other hand, as the sample thickness increases, the interaction becomes softer at high momenta, and our theory should become more accurate. To model this, we considered a particular interaction with a parameter $\Lambda = \lambda l$ related to sample thickness. I have presented a number of results at larger λ . In particular, the cutoff dependence becomes negligible at large λ , increasing our confidence in the results. Generally, we find that while the structure of minima found in the ME dispersions for the pure Coulomb case ($\lambda = 0.0$) persists at larger λ , the minima become shallower (and even disappear for $\frac{1}{3}$ around $\lambda = 3.0$), while the entire ME dispersion moves down in energy. We also find that the fraction of the spectral weight in the lowest mode decreases with sample thickness. Finally, we find that the $\frac{2}{5}$ incompressible state should become unstable somewhere around $\lambda_{cr} = 2.65$, while the $\frac{3}{7}$ incompressible state should disappear near $\lambda_{cr} = 2.4$. The instabilities are at finite wavevector, and one may speculate that the transition might be to a crystal phase⁴⁵. These are estimates for a clean system, and would be revised downwards for systems with disorder. Unfortunately, results from exact diagonalizations or other essentially exact methods are not currently available to test our results for thick samples.

Turning to the spin-flip MEs, we find good agreement between our results and exact diagonalizations⁴³ for the case $\nu = \frac{1}{3}$, even in the worst case $\lambda = 0.0$. We find that for $\frac{1}{3}$, the spin-wave mode is the lowest one, and is well separated from the other modes for small q , justifying its treatment as a quantum ferromagnet⁴¹. However, for $\nu = \frac{2}{5}$ we find that the lowest mode is *not* the spin-wave, but a spin-flip excitation that creates a hole in the $n = 1$ CF-LL, and puts a minority spin particle in the $n = 0$ CF-LL. This implies that a quantum ferromagnet treatment⁴¹ that ignores the CFs would be inadequate in this case. Furthermore, the lowest excitation has negative energy (in the absence of a Zeeman interaction) for a substantial range of q , with a minimum at finite wavevector. These predictions should be detectable in the spin structure factor, and in the temperature dependence of the magnetization of the polarized $\nu = \frac{2}{5}$ state.

The most significant deficiency in our treatment is the way we handle the constraints. Constraints are known

to be crucial^{14,23,25,52,53} for compressible systems such as $\nu = \frac{1}{2}$. Ideally, one would like to employ a conserving approximation⁵⁴ in which the constraint would be satisfied, such as the one carried out by Read for the compressible states²⁵. An LLL formulation for all the principal fractions valid at all q , which is algebraically consistent, and which agrees with our approach at small q , has recently been postulated by Shankar⁴⁹. This formulation is amenable to a conserving approximation, and would be the way to settle matters of principle. However, we presented several lines of reasoning to suggest that in using our $\bar{\rho}$ we are already building in many nontrivial renormalizations at tree level, and that the effect of constraints would be minimal. The formulation of Shankar⁴⁹ shares this philosophy, and provides a partial justification of our truncation of $\bar{\rho}$ (in the smallness of the higher order terms of $\bar{\rho}_{pref}$ ⁴⁹).

In conclusion, our dynamical theory of Composite Fermions gives a satisfactory approximate account of the low-energy excitations around the gapped FQH states, the magnetoexciton modes. In addition to reproducing previous results we find some surprising predictions. There are many directions in which one can take this approach. Perhaps the most important are the treatment of disorder⁶⁶, and an understanding of the crystal phase⁶⁷, which I hope to return to in future work.

VI. ACKNOWLEDGEMENTS

I would like to thank J.K.Jain, R.Shankar, S.H.Simon, and S.L.Sondhi for helpful conversations.

-
- ¹ D.Tsui, H.Stromer and A.Gossard, Phys. Rev. Lett. **48**, 1599, (1982).
 - ² R.B.Laughlin, Phys. Rev. Lett. **50**, 1395, (1983).
 - ³ B.I.Halperin, Phys. Rev. Lett. **52**, 1583 (1984); D.P.Arovas, J.R.Schreiffer, and F.Wilczek, Phys. Rev. Lett. **53**, 722 (1984).
 - ⁴ J.K.Jain, Phys. Rev. Lett. **63**, 199, (1989); Phys. Rev. **B** **41**, 7653 (1990); Science **266**, 1199 (1994).
 - ⁵ J.K.Jain and R.K.Kamilla, in Chapter 1 of "Composite Fermions", Olle Heinonen, Editor (World Scietific, Teaneck, NJ, 1998).
 - ⁶ For a review, see H.L.Stormer and D.C.Tsui in Chapter 10 of "Perspectives in Quantum Hall Effects", S.Das Sarma and A.Pinczuk editors (Wiley, New York, 1997).
 - ⁷ J.M.Leinaas and J.Myrheim, Nuovo Cimento **37B**, 1 (1977).
 - ⁸ S.M.Girvin, in Chapter 9 of "The Quantum Hall Effect", Edited by R.E.Prange and S.M Girvin, Springer-Verlag, 1990.
 - ⁹ S.M.Grivin and A.H.MacDonald, Phys. Rev. Lett. **58**, 1252 (1987).
 - ¹⁰ S.-C.Zhang, H.Hansson and S.A.Kivelson, Phys. Rev. Lett. **62**, 82, (1989); D.-H.Lee and S.-C.Zhang, Phys. Rev. Lett.

- 66**, 1220 (1991); S.-C.Zhang, Int. J. Mod. Phys., **B6**, 25 (1992).
- ¹¹ N.Read, Phys. Rev. Lett., **62**, 86 (1989).
- ¹² A.Lopez and E.Fradkin, Phys. Rev. B **44**, 5246 (1991), *ibid* **47**, 7080, (1993), Phys. Rev. Lett. **69**, 2126 (1992); For the latest review of the fermionic CS approach see A.Lopez and E.Fradkin in Chapter 3 of “Composite Fermions”, Olle Heinonen, Editor, (World Scietific, Teaneck, NJ, 1998).
- ¹³ V.Kalmeyer and S.-C.Zhang, Phys. Rev. B **46**, 9889 (1992).
- ¹⁴ B.I.Halperin, P.A.Lee and N.Read, Phys. Rev. B **47**, 7312 (1993).
- ¹⁵ R.Shankar and G.Murthy, Phys. Rev. Lett. **79**, 4437, (1997).
- ¹⁶ G.Murthy and R.Shankar, in Chapter 4 of “Composite Fermions”, Olle Heinonen, Editor, (World Scietific, Teaneck, NJ, 1998).
- ¹⁷ D.Bohm and D.Pines, Phys. Rev. **92**, 609, (1953).
- ¹⁸ S.H.Simon, A.Stern, and B.I.Halperin, Phys. Rev. B **54**, R11114 (1996).
- ¹⁹ S.H.Simon and B.I.Halperin, Phys. Rev. B **48**, 17368, (1993).
- ²⁰ N.Read, Semi. Sci. Tech. **9**, 1859 (1994); Surf. Sci., **361/362**, 7 (1996).
- ²¹ W.Kohn, Phys. Rev **123**, 1242 (1961).
- ²² S.M.Girvin, A.H.MacDonald and P.Platzman, Phys. Rev. B **33**, 2481, (1986).
- ²³ D.H.Lee, Phys. Rev. Lett. **80**, 4745 (1998).
- ²⁴ V.Pasquier and F.D.M.Haldane, Nucl. Phys. **B516**, 719 (1998).
- ²⁵ N.Read, Phys. Rev. **B58**, 16262 (1998).
- ²⁶ F.F.Fang and W.E.Howard, Phys. Rev. Lett. **16**, 797 (1966); T.Ando, A.B.Fowler, and F.Stern, Rev. Mod. Phys. **54**, 437 (1982).
- ²⁷ F.D.M.Haldane and E.H.Rezayi, Phys. Rev. Lett. **54**, 237 (1985).
- ²⁸ F.C.Zhang and S.Das Sarma, Phys. Rev. B **33**, 2903 (1986); D.Yoshioka, J. Phys. Soc. Jpn. **55**, 885 (1986); T.Chakraborty, P.Pietlainen, and F.C.Zhang, Phys. Rev. Lett, **57**, 130 (1986); R.Morf and B.I.Halperin, Z. Phys. B **68**, 391 (1987); R.Price and S.Das Sarma, Phys. Rev. B **54**, 8033 (1996).
- ²⁹ V.Melik-Alaverdian and N.E.Bonesteel, Phys. Rev. B **52**, R17032 (1995); V.Melik-Alaverdian, N.E.Bonesteel, and G.Ortiz, Phys. Rev. Lett., **79**, 5286 (1997).
- ³⁰ K.Park and J.K.Jain, Phys. Rev. Lett. **81**, 4200 (1998).
- ³¹ G.Murthy and R.Shankar, cond-mat 9806380, to appear in Phys. Rev. **B**.
- ³² G.Murthy, K.Park, R.Shankar, and J.K.Jain, Phys. Rev. **B58**, 13263 (1998).
- ³³ K.W.Chiu and J.J.Quinn, Phys. Rev. B **9**, 4724 (1974); N.Horing and M.Yildiz, Ann. Phys. NY **97**, 216 (1976); T.Theis, Surf. Sci. **98**, 515 (1980); P.Hawrylak and J.J.Quinn, Phys. Rev. **B31**, 6592 (1985); Yu.A.Bychkov, S.V.Iordanskii, and G.M.Eliashberg, JETP Lett. **33**, 152 (1981).
- ³⁴ C.Kallin and B.I.Halperin Phys. Rev B **30**, 5655, (1984).
- ³⁵ A.H.MacDonald, Jour. Phys. **C18**, 1003 (1985).
- ³⁶ H.C.A.Oji and A.H.MacDonald, Phys. Rev. **B33**, 3810 (1986); I.K.Marmorkos and S.Das Sarma, Phys. Rev. **B45**, 13396 (1992); J.P.Longo and C.Kallin, Phys. Rev. **B47**, 4429 (1993).
- ³⁷ N.d’Ambrunil and R.Morf, Phys. Rev. **B40**, 6108 (1989); P.M.Platzman and S.He, Phys. Rev. **B49**, 13674 (1994); S.He, S.H.Simon, and B.I.Halperin, Phys. Rev. **B50**, 1823 (1994); S.He and P.M.Platzman, Surf. Sci **361/362**, 87 (1996); S.He, Computers in Phys. **11**, 194 (1997).
- ³⁸ X.G.Wu and J.K.Jain, Phys. Rev. **B51**, 1752 (1995); R.K.Kamilla, X.G.Wu, and J.K.Jain, Phys. Rev. Lett. **76**, 1332 (1996); Phys. Rev. **B54**, 4873 (1996).
- ³⁹ S.H.Simon and B.I.Halperin, Phys. Rev. **B48**, 17368 (1993); S.H.Simon and B.I.Halperin, Phys. Rev. B **50**, 1807 (1994); X.C.Xie, Phys. Rev. **B49**, 16833 (1994).
- ⁴⁰ S.L.Sondhi, A.Karlhede, S.A.Kivelson, and E.H.Rezayi, Phys. Rev. **B47**, 16419 (1993).
- ⁴¹ N.Read and S.Sachdev, Phys. Rev. Lett. **75**, 3509 (1995); M.Kasner and A.H.MacDonald, Phys. Rev. Lett. **76**, 3204 (1996); C.Timm, S.M.Girvin, P.Henlius, and A.W.Sandvik, Phys. Rev. **B58**, 1464 (1998); M.Kasner, J.J.Palacios, and A.H.MacDonald, cond-mat 9808186.
- ⁴² R.Tycko, S.E.Barrett, G.Dabbagh, L.N.Pfeiffer, and K.W.West, Science **268**, 1460 (1995); S.E.Barrett, G.Dabbagh, L.N.Pfeiffer, K.W.West, and R.Tycko, Phys. Rev. Lett. **74**, 5112 (1995); M.J.Manfra, E.H.Aifer, B.B.Goldberg, D.A.Broido, L.N.Pfeiffer, and K.W.West, Phys. Rev. **B54**, 17327 (1996).
- ⁴³ T.Nakajima and H.Aoki, Phys. Rev. Lett. **73**, 3568 (1994).
- ⁴⁴ S.S.Mandal, Phys. Rev. **B56**, 7525 (1997).
- ⁴⁵ P.K.Lam and S.M.Girvin, Phys. Rev. **B30**, 473 (1984); D.Levesque, J.J.Weiss, and A.H.MacDonald, Phys. Rev. **B30**, 1056 (1984).
- ⁴⁶ R.K.Kamilla and J.K.Jain, Phys. Rev. **B55**, R13417 (1997).
- ⁴⁷ A.L.Fetter, C.B.Hanna, and R.B.Laughlin, Phys. Rev. B **39**, 9679 (1989); *ibid* **43**, 309 (1991); Q.Dai, J.L.Levy, A.L.Fetter, C.B.Hanna, and R.B.Laughlin, Phys. Rev. B **46**, 5642 (1992).
- ⁴⁸ I.V.Lerner and Yu.E.Loikov, Sov. Phys. JETP **57**, 588 (1980).
- ⁴⁹ R.Shankar, cond-mat 9903064.
- ⁵⁰ F.D.M.Haldane, in Chapter 8 of “The Quantum Hall Effect”, R.E.Prange and S.M.Girvin, Editors (Springer-Verlag, New York, 1990).
- ⁵¹ G.Dev and J.K.Jain, Phys. Rev. Lett. **69**, 2843 (1992).
- ⁵² B.I.Halperin and A.Stern, Phys. Rev. Lett. **80**, 5457 (1998); G.Murthy and R.Shankar, *ibid* 5458 (1998).
- ⁵³ A.Stern, B.I.Halperin, F.von Oppen, and S.H.Simon, cond-mat 9812135.
- ⁵⁴ G.Baym and L.P.Kadanoff, Phys. Rev. **124**, 287 (1961).
- ⁵⁵ G.Rickayzen, Phys. Rev. **115**, 795 (1957).
- ⁵⁶ R.H.Morf, cond-mat 9812181. Morf raises the possibility that the values of λ used in ref.³⁰ to compare to the experimental numbers or ref.⁵⁷, are incorrect due to errors in ref.⁵⁸. He suggests that the physical values of λ are between 1 and 1.5.
- ⁵⁷ R.R.Du, H.L.Störmer, D.C.Tsui, L.N.Pfeiffer, and K.W.West, Phys. Rev. Lett. **70**, 2944 (1993).
- ⁵⁸ M.W.Ortalano, S.He, and S.Das Sarma, Phys. Rev. **B55**, 7702 (1997).
- ⁵⁹ K.Moon, H.Mori, K.Yang, S.M.Girvin, A.H.MacDonald, L.Zheng, D.Yoshioka, and S.-C.Zhang, Phys. Rev. **B51**, 5138 (1995).
- ⁶⁰ B.I.Halperin, Helv. Phys. Acta **556**, 75 (1983).
- ⁶¹ A.Lopez and E.Fradkin, Phys. Rev. **B51**, 4347 (1995).

- ⁶² K.Yang, K.Moon, L.Zheng, A.H.MacDonald, S.M.Girvin, D.Yoshioka, and S.-C.Zhang, Phys. Rev. Lett. **72**, 732 (1994); For a review, see S.M.Girvin in Chapter 5 of “Perspectives in Quantum Hall Effects”, S.Das Sarma and A.Pinczuk editors (Wiley, New York, 1997).
- ⁶³ For a review of the experiments, see J.P.Eisenstein in Chapter 2 of “Perspectives in Quantum Hall Effects”, S.Das Sarma and A.Pinczuk editors (Wiley, New York, 1997).
- ⁶⁴ K.Park and J.K.Jain, Phys. Rev. Lett. **80**, 4237 (1998).
- ⁶⁵ R.R.Du, A.S.Yeh, H.L.Stormer, D.C.Tsui, L.N.Pfeiffer, and K.W.West, Phys. Rev. Lett. **75**, 3926 (1995).
- ⁶⁶ R.B.Laughlin, M.L.Cohen, J.M.Kosterlitz, H.Levine, S.B.Libby and A.M.M.Pruisken, Phys. Rev. **B32**, 1311 (1985); A.H.MacDonald, K.L.Liu, S.M.Girvin, and P.M.Platzman, Phys. Rev. **B33**, 4014 (1986).
- ⁶⁷ For a review see H.A.Fertig in Chapter 3 of “Perspectives in Quantum Hall Effects”, S.Das Sarma and A.Pinczuk editors (Wiley, New York, 1997).